JCI The Journal of Clinical Investigation

Modulation of subthalamic T-type Ca^{2+} channels remedies locomotor deficits in a rat model of Parkinson disease

Chun-Hwei Tai, … , Chen-Syuan Huang, Chung-Chin Kuo

J Clin Invest. 2011;121(8):3289-3305. https://doi.org/10.1172/JCI46482.

Research Article Neuroscience

An increase in neuronal burst activities in the subthalamic nucleus (STN) is a well-documented electrophysiological feature of Parkinson disease (PD). However, the causal relationship between subthalamic bursts and PD symptoms and the ionic mechanisms underlying the bursts remain to be established. Here, we have shown that T-type Ca^{2+} channels are necessary for subthalamic burst firing and that pharmacological blockade of T-type Ca^{2+} channels reduces motor deficits in a rat model of PD. Ni^{2+}, mibefradil, NNC 55-0396, and efonidipine, which inhibited T-type Ca^{2+} currents in acutely dissociated STN neurons, but not Cd^{2+} and nifedipine, which preferentially inhibited L-type or the other non–T-type Ca^{2+} currents, effectively diminished burst activity in STN slices. Topical administration of inhibitors of T-type Ca^{2+} channels decreased in vivo STN burst activity and dramatically reduced the locomotor deficits in a rat model of PD. Cd^{2+} and nifedipine showed no such electrophysiological and behavioral effects. While low-frequency deep brain stimulation (DBS) has been considered ineffective in PD, we found that lengthening the duration of the low-frequency depolarizing pulse effectively improved behavioral measures of locomotion in the rat model of PD, presumably by decreasing the availability of T-type Ca^{2+} channels. We therefore conclude that modulation of subthalamic T-type Ca^{2+} currents and consequent burst discharges may provide new strategies for the treatment of PD.

Modulation of subthalamic T-type Ca^{2+} channels remedies locomotor deficits in a rat model of Parkinson disease

Chun-Hwei Tai,[1,2] Ya-Chin Yang,[3,4] Ming-Kai Pan,[1,2] Chen-Syuan Huang,[4] and Chung-Chin Kuo[1,2]

[1]Department of Physiology, National Taiwan University College of Medicine, Taipei, Taiwan. [2]Department of Neurology, National Taiwan University Hospital, Taipei, Taiwan. [3]Department of Biomedical Sciences, and [4]Graduate Institute of Biomedical Sciences, Chang Gung University, Tao-Yuan, Taiwan.

An increase in neuronal burst activities in the subthalamic nucleus (STN) is a well-documented electrophysiological feature of Parkinson disease (PD). However, the causal relationship between subthalamic bursts and PD symptoms and the ionic mechanisms underlying the bursts remain to be established. Here, we have shown that T-type Ca^{2+} channels are necessary for subthalamic burst firing and that pharmacological blockade of T-type Ca^{2+} channels reduces motor deficits in a rat model of PD. Ni^{2+}, mibefradil, NNC 55-0396, and efonidipine, which inhibited T-type Ca^{2+} currents in acutely dissociated STN neurons, but not Cd^{2+} and nifedipine, which preferentially inhibited L-type or the other non–T-type Ca^{2+} currents, effectively diminished burst activity in STN slices. Topical administration of inhibitors of T-type Ca^{2+} channels decreased in vivo STN burst activity and dramatically reduced the locomotor deficits in a rat model of PD. Cd^{2+} and nifedipine showed no such electrophysiological and behavioral effects. While low-frequency deep brain stimulation (DBS) has been considered ineffective in PD, we found that lengthening the duration of the low-frequency depolarizing pulse effectively improved behavioral measures of locomotion in the rat model of PD, presumably by decreasing the availability of T-type Ca^{2+} channels. We therefore conclude that modulation of subthalamic T-type Ca^{2+} currents and consequent burst discharges may provide new strategies for the treatment of PD.

Introduction

Parkinson disease (PD) is closely related to aberrant cortico-basal ganglia loop functions in a state of dopamine deficiency (1, 2). The subthalamic nucleus (STN) has been proposed to play a key role in the abnormal functioning of the basal ganglia circuitry in PD (3). Increased burst firings of STN have been implicated as one of the pathognomonic electrophysiological features associated with PD (3–8). Although it remains unexplored whether the increased burst activity in STN has a direct casual relationship to parkinsonian motor disabilities, either lesion of STN or delivery of electrical currents at high frequency into STN could relieve most motor symptoms in primate PD models (9, 10). Accordingly, deep brain stimulation (DBS) of STN (and other nuclei) has become an established treatment of PD-related motor symptoms in neurological clinics (11–14). In theory, DBS may involve modulation of the STN firing pattern and thus cortico-basal ganglia loop function. However, the exact mechanism underlying DBS is so far not clear (15), which precludes a more sophisticated or rational adjustment of the stimulation parameters for a better clinical outcome.

Isolated neurons of STN are capable of spontaneous repetitive single-spike firing (16, 17), suggesting that they are intrinsically programmed for repetitive discharges. The ionic mechanisms underlying the spontaneous single-spike activities of STN may involve resurgent or persistent Na^+ channels and Ca^{2+}-dependent K^+ conductance (16–19). The single-spiking STN neurons could be readily switched to another firing mode characterized by semirhythmic bursts induced by membrane hyperpolarization, a condition that may occur with decreased dopamine, as in PD (16, 17, 20–25). However, the ionic mechanism underlying the switch is not clear. In thalamic relay neurons, which are evolutionarily closely related to STN neurons, burst firings are associated with hyperpolarization-driven recovery of low voltage–activated (LVA) T-type Ca^{2+} conductance from inactivation (26). Although there was a report of subthalamic Ni^{2+}-sensitive Ca^{2+} currents in brain slices that may give a low-threshold spike following membrane hyperpolarization (18, 27), another study failed to obtain T-type Ca^{2+} conductance in acutely dissociated STN neurons (28).

Here we report that the T-type Ca^{2+} channel is an essential element for subthalamic burst activity both in vitro and in vivo. Moreover, T-type Ca^{2+} channel blockers not only successfully inhibit the burst activity in STN but also readily remedy the locomotor deficits in parkinsonian rats. These data provide direct evidence that T-type Ca^{2+} channels are essential for the genesis of the burst discharges in STN, and thus may play a pivotal role in the locomotor abnormalities of PD. The results are indicative of what we believe to be a novel and promising perspective for the treatment of PD.

Results

Electrophysiological and pharmacological studies support the existence of LVA Ca^{2+} channels in acutely dissociated STN neurons. In view of the previous controversy over the existence of T-type Ca^{2+} channels in subthalamic neurons (18, 27, 28), we first characterized Ca^{2+} currents in acutely dissociated STN neurons. Immediately after the establishment of whole-cell configuration, most acutely dissociated subthalamic neurons showed both LVA (T-type) and high voltage–activated (HVA) components of Ca^{2+} currents. However, especially in the absence of the "regenerative" composition (i.e., MgATP, NaGTP, and $NaPO_4$ creatine) in the internal solution, HVA

Authorship note: Chun-Hwei Tai and Ya-Chin Yang contributed equally to this work.

Conflict of interest: The authors have declared that no conflict of interest exists.

Citation for this article: *J Clin Invest.* 2011;121(8):3289–3305. doi:10.1172/JCI46482.

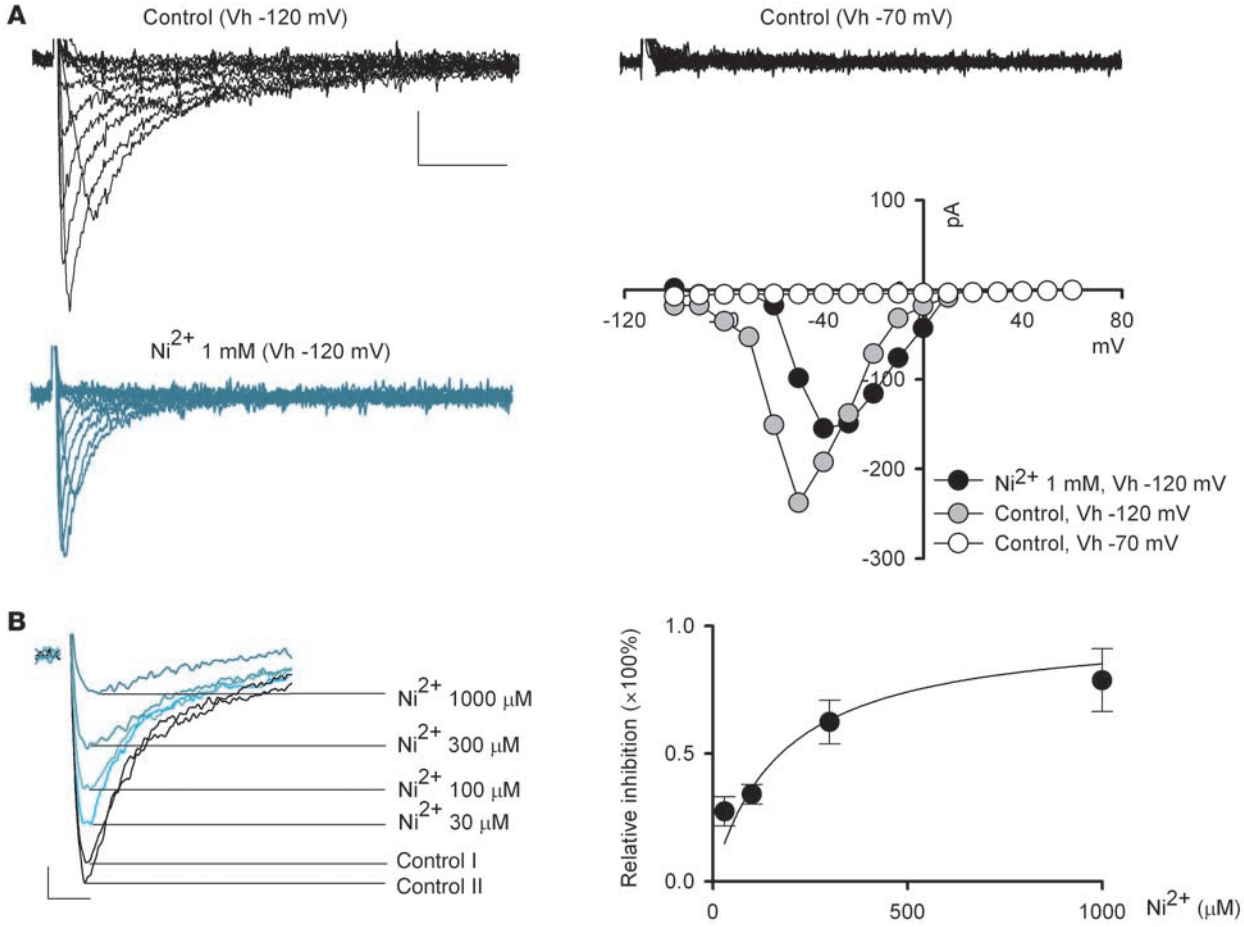

Figure 1

Electrophysiological characterization of and effect of Ni^{2+} on LVA Ca^{2+} currents in acutely dissociated subthalamic neurons. (**A**) Representative "pure" voltage-dependent LVA Ca^{2+} currents recorded from a subthalamic neuron. The same neuron is stepped from a holding potential (Vh) of –120 mV or –70 mV to different test voltages (–100 to +60 mV) to elicit Ca^{2+} currents in the absence (control, black traces) or presence (blue traces) of 1 mM Ni^{2+}. The HVA Ca^{2+} currents are apparently absent in this cell and in the recording condition. The current-voltage relationship of the shown currents is also plotted. Scale bars: 50 pA/20 ms for all traces in **A**. (**B**) LVA Ca^{2+} currents elicited at –50 mV from a holding potential of –120 mV are recorded in the absence (black traces) and presence (colored traces) of 30, 100, 300, or 1,000 μM Ni^{2+} in the same neuron. Two control currents (Control I and Control II) were obtained before and after application of different concentrations of Ni^{2+}. The average Ni^{2+} inhibitory effect on LVA Ca^{2+} currents is plotted on the right. The curve is a fit based on a one-to-one binding reaction and is of the form: relative inhibition = $([Ni^{2+}]/175\ \mu M)/[1 + ([Ni^{2+}]/175\ \mu M)]$. n = 4, 5, 6, and 4 for 30, 100, 300, and 1,000 μM Ni^{2+}, respectively. Scale bars: 25 pA/5 ms.

currents usually run down fast, and frequently only LVA currents would remain in a subthalamic neuron after approximately 5 minutes. Figure 1A shows an example of the "pure" voltage-dependent LVA Ca^{2+} currents recorded from a dissociated STN neuron, where the HVA non-inactivating Ca^{2+} currents are apparently absent. The Ca^{2+} currents could be elicited by step depolarization from a holding potential of –120 mV to –80 mV (see also the gray symbols in the current-voltage plot, Figure 1A). The elicited macroscopic Ca^{2+} currents showed fast inactivation with a saturating decay time constant of approximately 10–15 ms at more positive potentials. In addition, a holding potential of –70 mV was sufficient to completely wipe out the currents (Figure 1A, upper right traces). These electrophysiological findings revealed characteristics typical of Ca_v 3.1 and/or Ca_v3.2 LVA channels (29) and are consistent with the previous report of significant expression of Ca_v 3.1 channels in the STN of human brain (ref. 30 and also see below). We then examined the subthalamic Ca^{2+} currents pharmacologically. We first studied the effect of Ni^{2+} and mibefradil, two widely used T-channel inhibitors (31, 32). Consistent with previous reports for T-type Ca^{2+} channels (33), 1 mM Ni^{2+} inhibited the isolated LVA Ca^{2+} currents in a voltage-dependent manner (Figure 1A). Figure 1B shows concentration-dependent inhibition of LVA currents by Ni^{2+}. Assuming a one-to-one binding action, Ni^{2+} bound to the LVA channel with an apparent dissociation constant of approximately 175 μM (Figure 1B), which is close to the IC_{50} of Ni^{2+} reported for Ca_v 3.1 channels (using Ca^{2+} at a physiological concentration as charge carrier) (34). Consistent with the role of mibefradil as an effective and selective organic blocker of T-type Ca^{2+} channels, Figure 2A shows that 3 μM mibefradil markedly decreased the LVA component of Ca^{2+} currents, but did not reduce the HVA Ca^{2+} currents in the same neuron. Mibefradil had a concentration-dependent inhibitory effect on isolated LVA Ca^{2+} currents, with an IC_{50} (1–3 μM, Figure 2A)

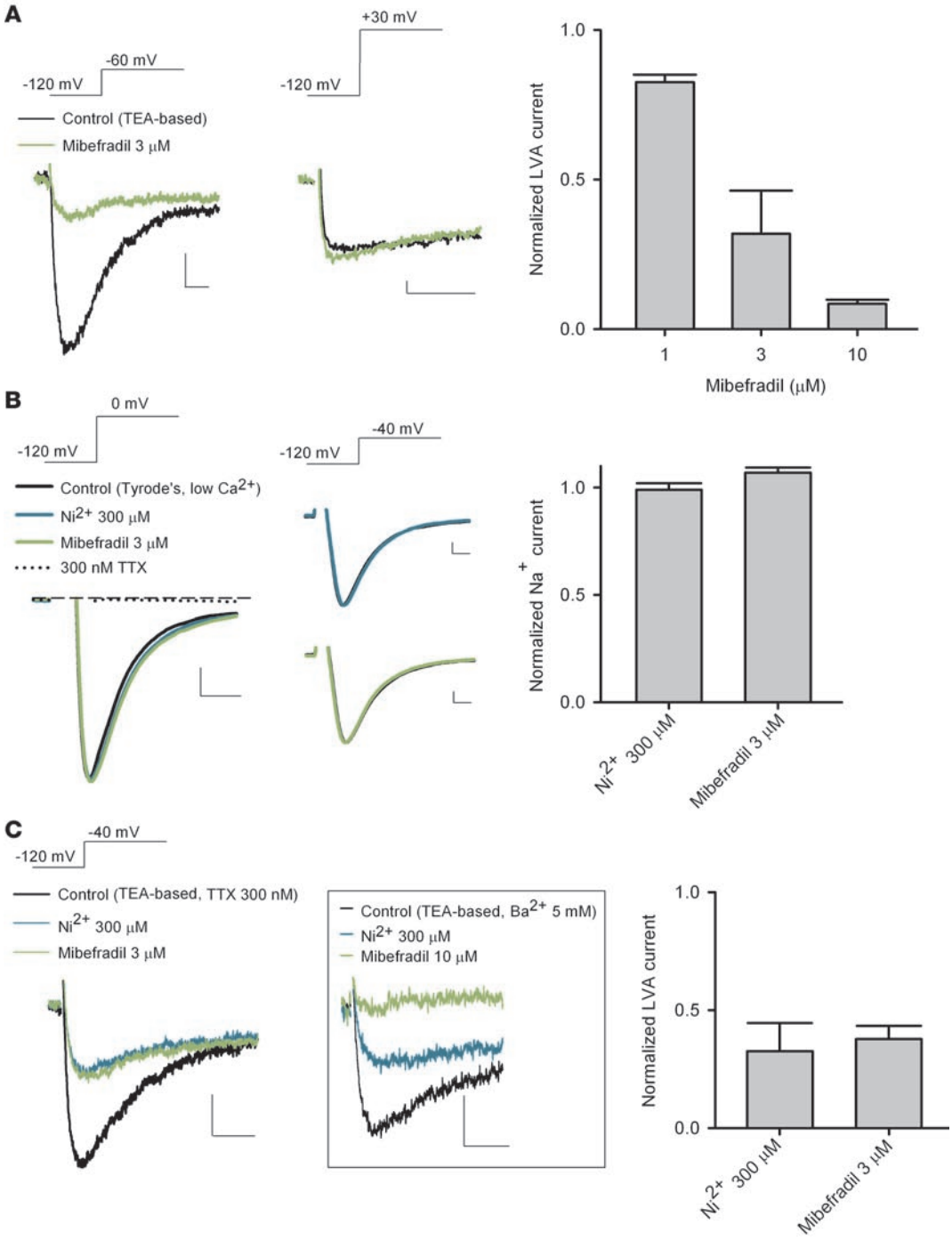

Figure 2

Effect of mibefradil (green traces) and Ni^{2+} (blue traces) on Ca^{2+} and Na^{+} currents in dissociated STN neurons. The holding potential is –120 mV. (**A**) Representative currents show that 3 μM mibefradil dramatically inhibits the Ca^{2+} current elicited at –60 mV (left panel) but has little inhibitory effect on that elicited at +30 mV (middle panel) in the same neuron. The peak LVA Ca^{2+} current amplitude (elicited at –60 mV) in the presence of drug is normalized to that in control to give the average inhibitory effect of 1–10 μM mibefradil (right panel, $n = 4$). Scale bars: 20 pA/20 ms. (**B**) 300 μM Ni^{2+} and 3 μM mibefradil lack an effect on subthalamic neuronal Na^{+} currents that are either elicited at 0 mV (and abolished by 300 nM TTX; left panel) or elicited at –40 mV (middle panel). In this experiment, the external TEA-based solution is replaced by a low-calcium Tyrode's solution (see Methods). The Na^{+} current (elicited at 0 mV) in the presence of drug is normalized to that in control to show the average drug effects (right panel, each $n = 4$). The dashed line indicates zero current level. Scale bars: 500 pA/0.5 ms. (**C**) Inhibition of LVA Ca^{2+} currents by 300 μM Ni^{2+} and 3 μM mibefradil with the addition of 300 nM TTX in the external TEA-based solution. The normalized Ca^{2+} current to the control is plotted to show the averaged effects (right panel, $n = 4$). The box shows the same inhibition of LVA currents by Ni^{2+} and mibefradil if 5 mM Ca^{2+} is replaced by 5 mM Ba^{2+} in the external TEA-based solution. Scale bars: 50 pA/20 ms.

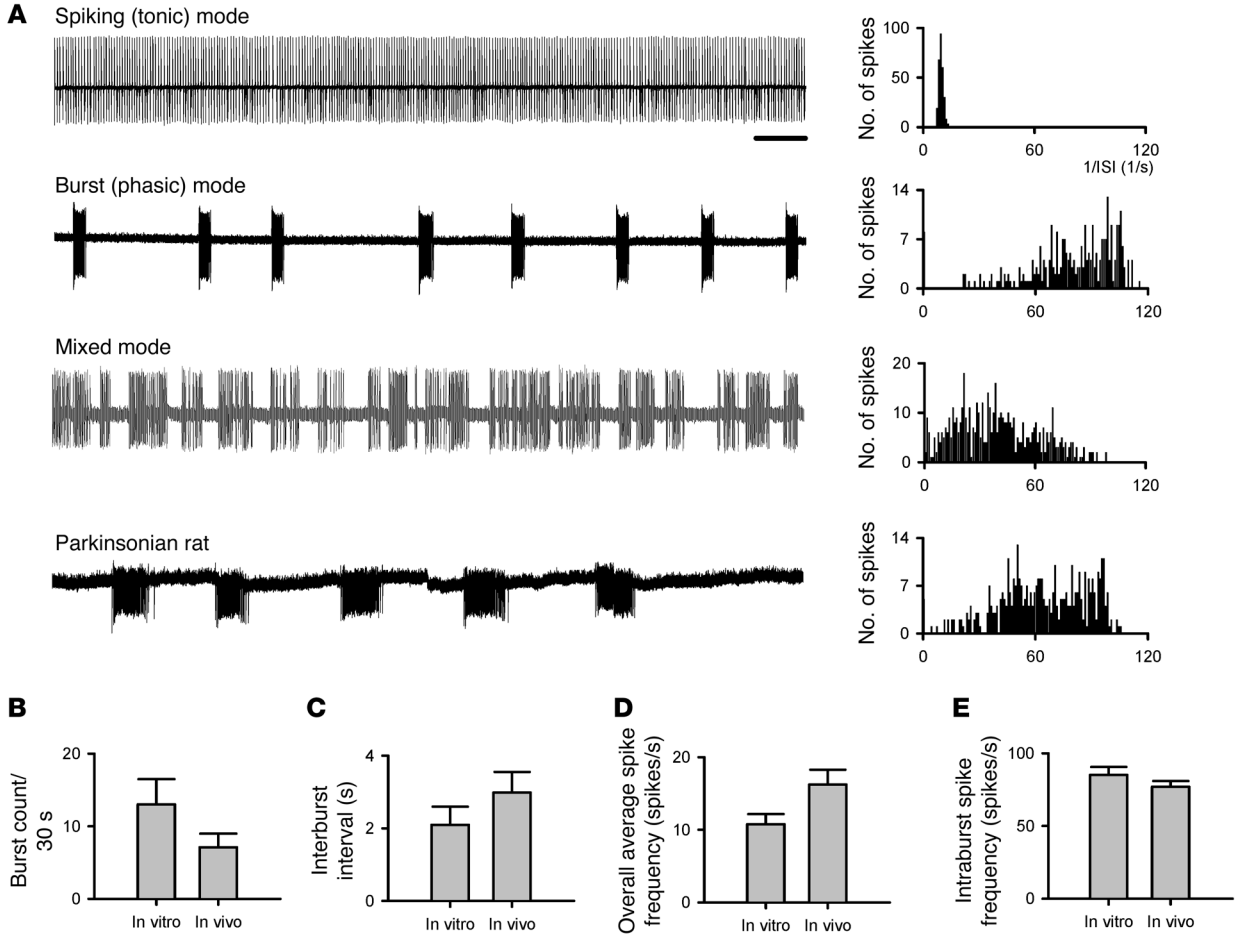

Figure 3

Spontaneous firing activities of subthalamic neurons in acute brain slices. (**A**) Examples of cell-attached patch-clamp recordings of spontaneous subthalamic discharges in acute brain slices of normal mice and of parkinsonian rats (each sweep represents a 30-second recording). Subthalamic neurons in normal mice may exhibit spiking (tonic), burst (phasic), or mixed patterns of firing, whereas the neurons in parkinsonian rats tend to be either silent or firing in bursts with longer intra-burst duration. The corresponding histogram plot for each of the sample traces is presented on the right end of each trace. The histogram plot shows a clear peak in the inverse of the inter-spike interval (ISI) for the spiking (tonic) firing, representing regular spikes at a frequency of approximately 10 Hz. In contrast, there is a smear in the higher frequencies plus a single peak at an extremely low frequency for the burst firing mode, consistent with periodic occurrence of irregular but high-frequency bursts of discharges. Scale bar: 2 seconds. (**B**–**E**) Comparison of different parameters of STN firing recorded from acute slices (in vitro, $n = 6$) with those from in vivo single-unit recording data (taken from Figures 7 and 8). $P = 0.24$, 0.53, 0.31, and 0.41 for **B**, **C**, **D**, and **E**, respectively.

also similar to that reported previously for Ca_v 3.1 channels (35). On the other hand, macroscopic Na^+ currents were unaffected by 3 μM mibefradil or 300 μM Ni^{2+} (Figure 2B). Also, the inhibition of LVA Ca^{2+} currents by either mibefradil or Ni^{2+} remained quantitatively similar with the addition of either 300 nM TTX or Ba^{2+} (in place of Ca^{2+}) as charge carrier (Figure 2C, compared with Figure 1B and Figure 2A). These electrophysiological and pharmacological characterizations demonstrate the presence of (probably Ca_v 3.1) LVA Ca^{2+} channels, and a specific inhibitory effect of Ni^{2+} and mibefradil on LVA Ca^{2+} rather than Na^+ currents in acutely dissociated STN neurons (also see below).

Inhibition of LVA Ca^{2+} channels abolishes burst discharges of STN neurons in acute brain slices. It is well documented that in the thalamus, a structure ontogenetically closely related to STN, the burst mode of neuronal discharge is critically dependent on the availability of T-type Ca^{2+} channels (26). Based on the findings in dissociated neurons, we took advantage of the same pharmacological tools to dissect their effects on the firing patterns of STN. We first performed extracellular patch recordings of STN neurons in acute mouse brain slices and then single-unit extracellular recording in intact animals for comparison (see below). We found 3 distinct modes of spontaneous activities in STN neurons in brain slices. Similar to previous reports (36), approximately 70% of neurons fired in a purely tonic pattern of single spikes (spiking mode), whereas approximately 20% of neurons fired in a characteristic burst pattern (burst mode). Only approximately 10% of neurons showed a mixed mode of firing ($n = 50$, Figure 3A). For comparison, we also recorded from acute slices of parkinsonian rats (see below), where we found that STN neurons either were silent or fired in bursts with longer burst duration than those found in vivo (Figure 3A, bottom trace, and see below). Histograms of the inverse of the interspike interval displayed distinct patterns for the 3 firing modes

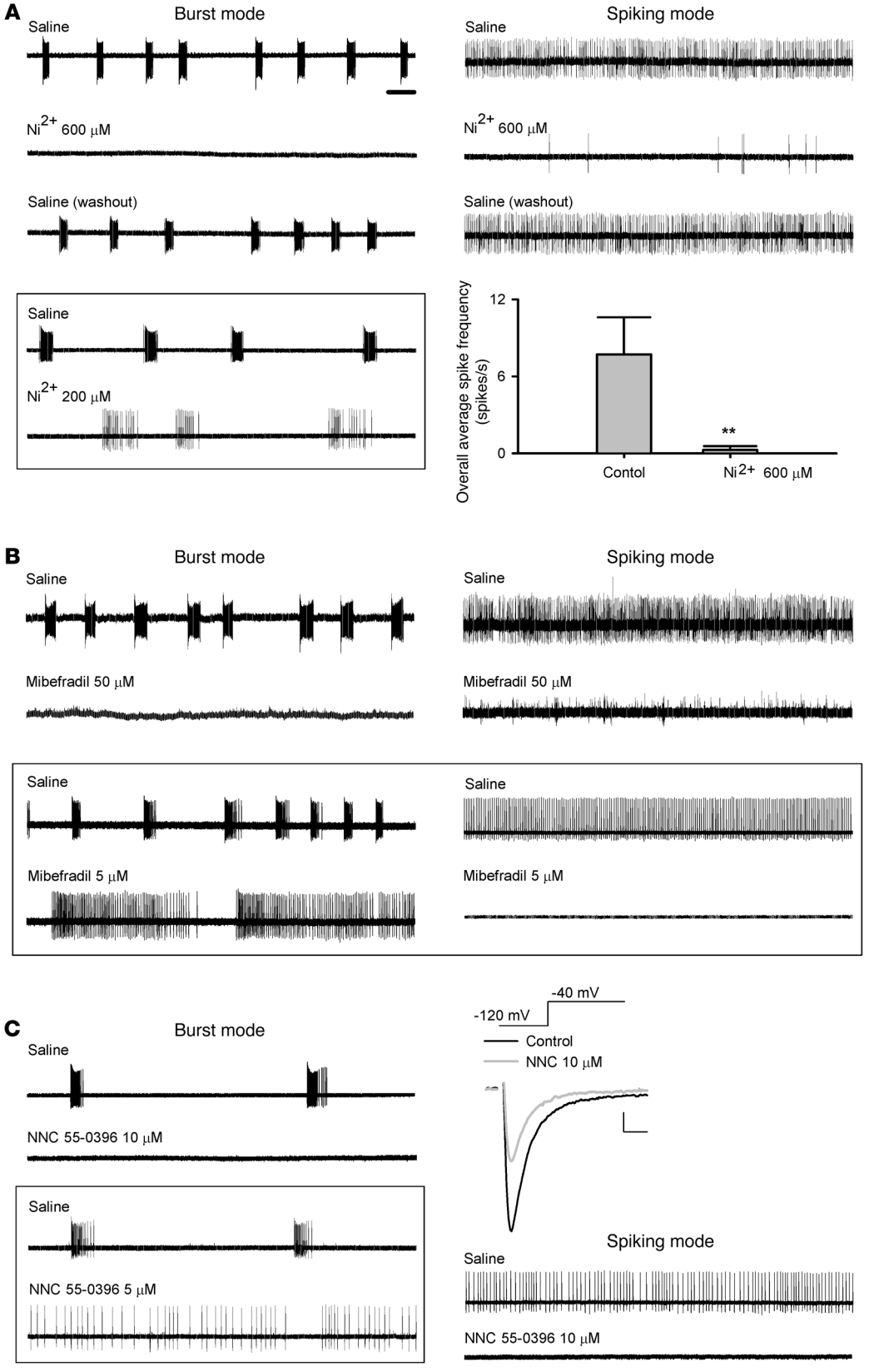

Figure 4

Attenuation of spontaneous burst and spiking discharges of STN by Ni^{2+}, mibefradil, and NNC 55-0396 in acute slices. Scale bar: 2 seconds, for all firing traces in this figure. (**A**) Left: 600 μM Ni^{2+} abolishes discharges in a cell that fires spontaneously in a burst mode. The effect of Ni^{2+} can be readily washed out by reperfusion of saline. The data in the boxed panel show that lower concentrations of Ni^{2+} (e.g., 200 μM) would attenuate bursts and turn the cell fired in a more spiking pattern. Right: The spontaneous spiking firing can also be inhibited by 600 μM Ni^{2+} and readily washed out by saline. The overall average spike frequency is robustly decreased by 600 μM Ni^{2+} (n = 5, $^{**}P < 0.005$). (**B**) 50 μM mibefradil wipes out both burst and spiking discharges of STN. The data in the boxed panel show that 5 μM mibefradil turns the phasic bursts into spiking discharges. (**C**) 5–10 μM NNC 55-0396 shows effects similar to those of Ni^{2+} and mibefradil. The representative currents show inhibition of LVA currents (elicited at –40 mV from a holding potential of –120 mV) by 10 μM NNC 55-0396. Scale bars: 100 pA/2 ms.

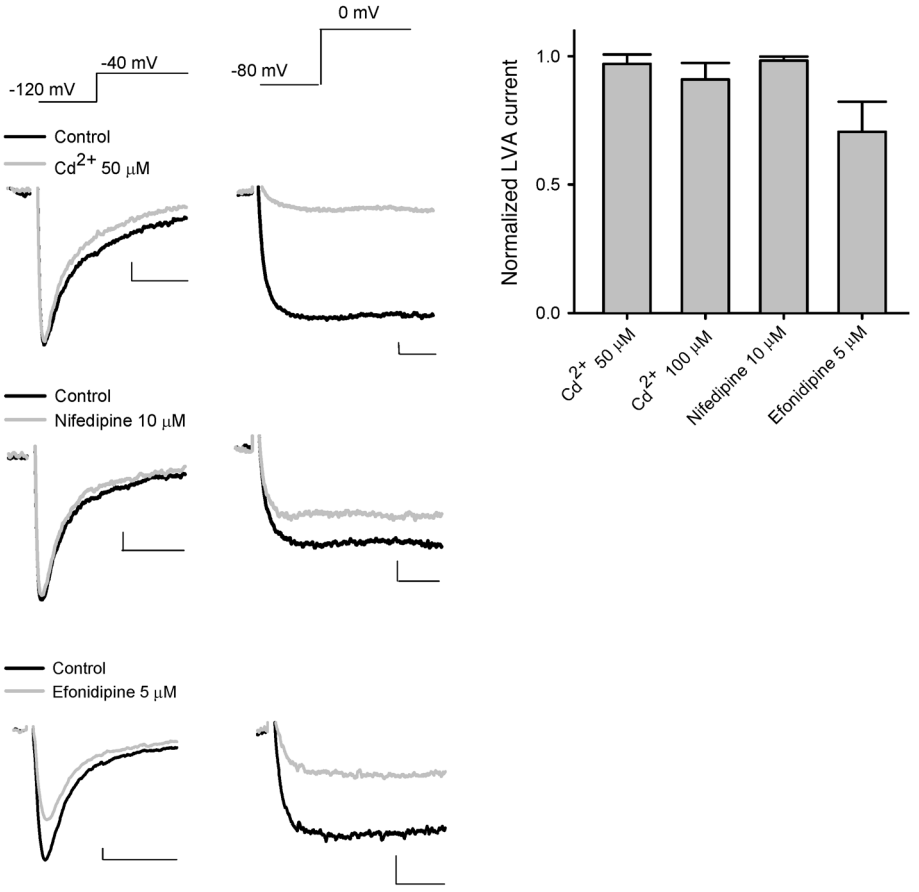

Figure 5
Effect of Cd^{2+}, nifedipine, and efonidipine on Ca^{2+} currents in dissociated STN neurons. 50 μM Cd^{2+} (upper traces) and 10 μM nifedipine (middle traces) both show little inhibition of LVA Ca^{2+} current (elicited at –40 mV from a holding potential of –120 mV; left) yet substantial inhibition of HVA Ca^{2+} current (elicited at 0 mV from a holding potential of –80 mV; middle) in the same dissociated STN neuron. 5 μM efonidipine (lower traces) exerts substantial inhibition of both LVA (left) and HVA (right) Ca^{2+} currents in the same neuron. The average inhibitory effect on LVA Ca^{2+} currents (elicited at –40 mV) by 50 μM Cd^{2+} (n = 5), 100 μM Cd^{2+} (n = 4), 10 μM nifedipine (n = 4), and 5 μM efonidipine (n = 4) is shown in the right panel. Scale bars: 50 pA/5 ms.

(Figure 3A, right panels). We analyzed these in vitro data using the same criteria as for the analysis of spike trains in in vivo recordings (see below and Methods for details). The results well matched those from in vivo recordings in terms of the burst count, the inter-burst interval, the overall average spike frequency, and the intra-burst spike frequency (Figure 3, B–E, and see below). We found that Ni^{2+} or mibefradil, which preferentially inhibits T-type Ca^{2+} currents in dissociated STN neurons, could attenuate bursts and/or transform firing from the burst to the spiking mode in acute STN slices if the concentrations were relatively low. With higher concentrations, Ni^{2+} and mibefradil wiped out both spiking and burst firings (Figure 4, A and B). We also tested NNC 55-0396, which was reported as a very specific T-channel inhibitor (37–39). NNC 55-0396 inhibited LVA Ca^{2+} currents, turned burst into spiking discharges at low concentration, and wiped out both spiking and burst discharges at high concentration in STN neurons in vitro, all of which were very similar to the effects of Ni^{2+} and mibefradil (Figure 4C).

Cd^{2+} and nifedipine have little inhibitory effect on either LVA Ca^{2+} currents and burst discharges of STN neurons in vitro. We then characterized the effects of pharmacological agents that are selective for HVA Ca^{2+} channels rather than LVA channels. Although Cd^{2+} may inhibit both HVA and LVA Ca^{2+} channels in very high concentrations, it has much higher affinity toward HVA than LVA channels. Thus, the quantitative difference between the effects of Cd^{2+} and Ni^{2+} may still provide important information for the identification of specific Ca^{2+} channels. For the sake of a more reliable comparison, we first isolated Ca^{2+} currents in terms of their electrophysiological properties. LVA Ca^{2+} currents were elicited at a "low" voltage of –40 mV from a holding potential of –120 mV, whereas HVA Ca^{2+} currents were elicited at a "high" voltage of 0 mV from a holding potential of –80 mV, which should inactivate most LVA channels (Figure 5). Fifty to 100 μM Cd^{2+} did not have a significant effect on the amplitude of LVA Ca^{2+} currents despite its robust inhibitory effect on HVA Ca^{2+} currents in the same neuron. The effects of Cd^{2+} were again quantitatively consistent with the involvement of Ca_v 3.1 channels (the IC_{50} of Cd^{2+} is ~700 μM) (40) rather than Ca_v 3.2 channels (the IC_{50} of Cd^{2+} is ~200 μM) (41), reminiscent of the electrophysiological findings with Ni^{2+} and mibefradil (Figures 1 and 2). Also, the effect of 10 μM nifedipine, a relatively specific blocker for the L-type Ca^{2+} channel, was qualitatively very similar to that of Cd^{2+}, and it had little inhibitory effect on the electrophysiologically isolated LVA Ca^{2+} currents. On the other hand, 5 μM efonidipine, a mixture of R(–)- and S(+)-enantiomers and a blocker selective for both T- and L-type Ca^{2+} channels but without a significant effect on N-, P/Q-, and R-type Ca^{2+} currents (42, 43), inhibited both LVA and HVA Ca^{2+} currents (Figure 5; see also Figure 6C for the effects of 20 μM efonidipine on LVA Ca^{2+} currents and Na^+ currents). We then compared the effect of Cd^{2+}, nifedipine, and efonidipine with that of selective T-channel inhibitors (Figure 4) on the firing pattern of STN neurons in brain slices. Neither nifedipine nor Cd^{2+} at a concentration that reduces HVA but not LVA Ca^{2+} currents showed an inhibitory effect on the burst activities of STN neurons (and Cd^{2+} even showed an increase in the tendency of bursts; Figure 6, A and B). On the other hand, efonidipine readily transformed firing from burst to spiking mode in a concentration-dependent manner, but showed no significant effect on

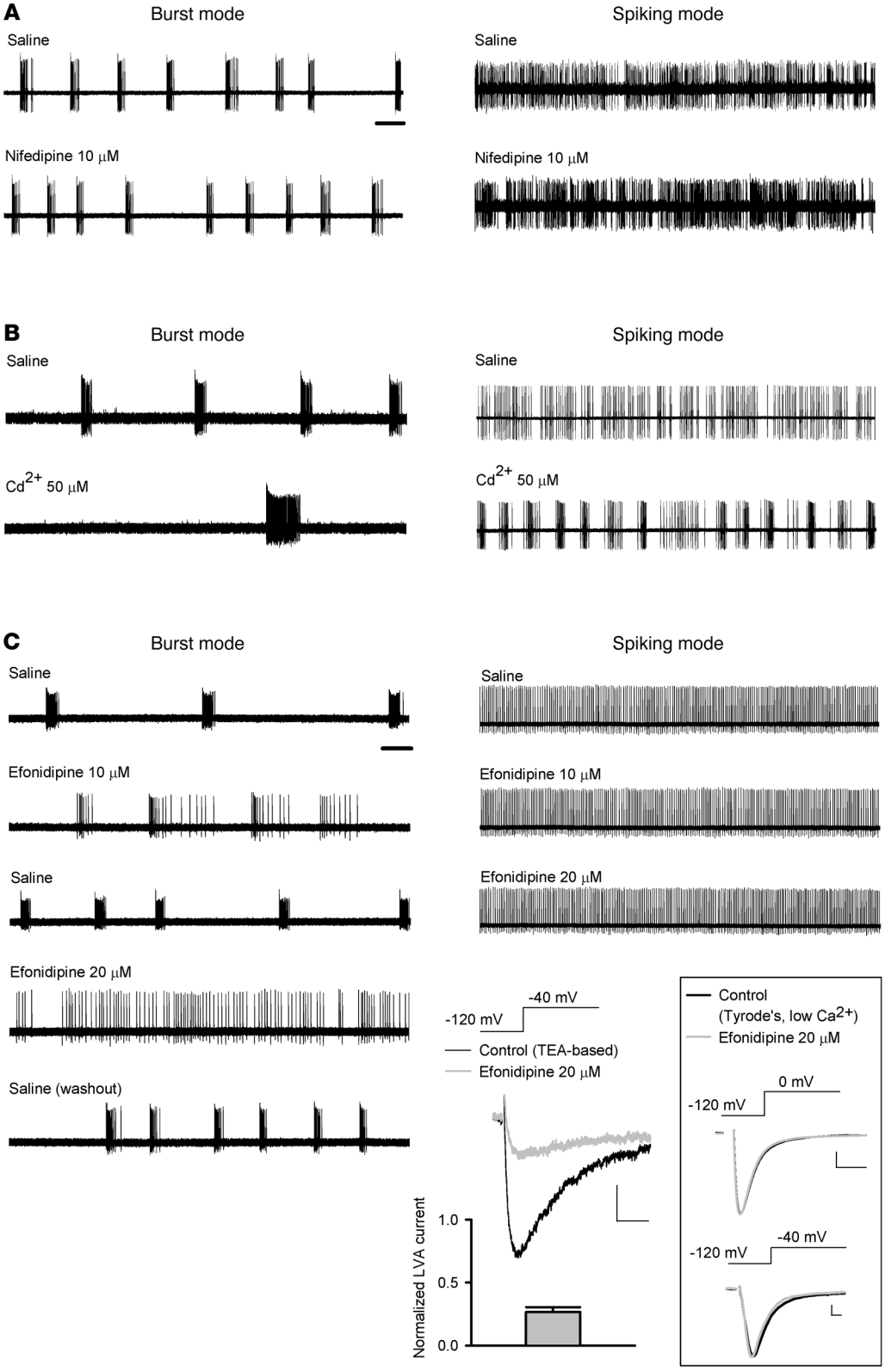

Figure 6
The effect of Cd^{2+}, nifedipine, and efonidipine on spontaneous burst and spiking discharges in acute STN slices. Scale bar: 2 seconds. 10 μM nifedipine (**A**) and 50 μM Cd^{2+} (**B**) show little inhibition on spontaneous firing of STN. (**C**) Efonidipine changes the spontaneous burst to spiking discharges in a concentration-dependent manner (left panel). On the other hand, the spontaneous spiking discharges are not affected by the same concentrations of efonidipine (right). The bottom right traces show manifest inhibition of LVA Ca^{2+} currents (elicited at –40 mV from a holding potential of –120 mV) by 20 μM efonidipine (n = 4). Scale bars: 50 pA/20 ms. The data in the boxed panel show that 20 μM efonidipine has little effect on subthalamic Na^{+} currents that are elicited either at 0 mV (upper panel) or at –40 mV (lower panel; the experimental conditions are the same as those described in Figure 2B). Scale bars: 500 pA/1 ms.

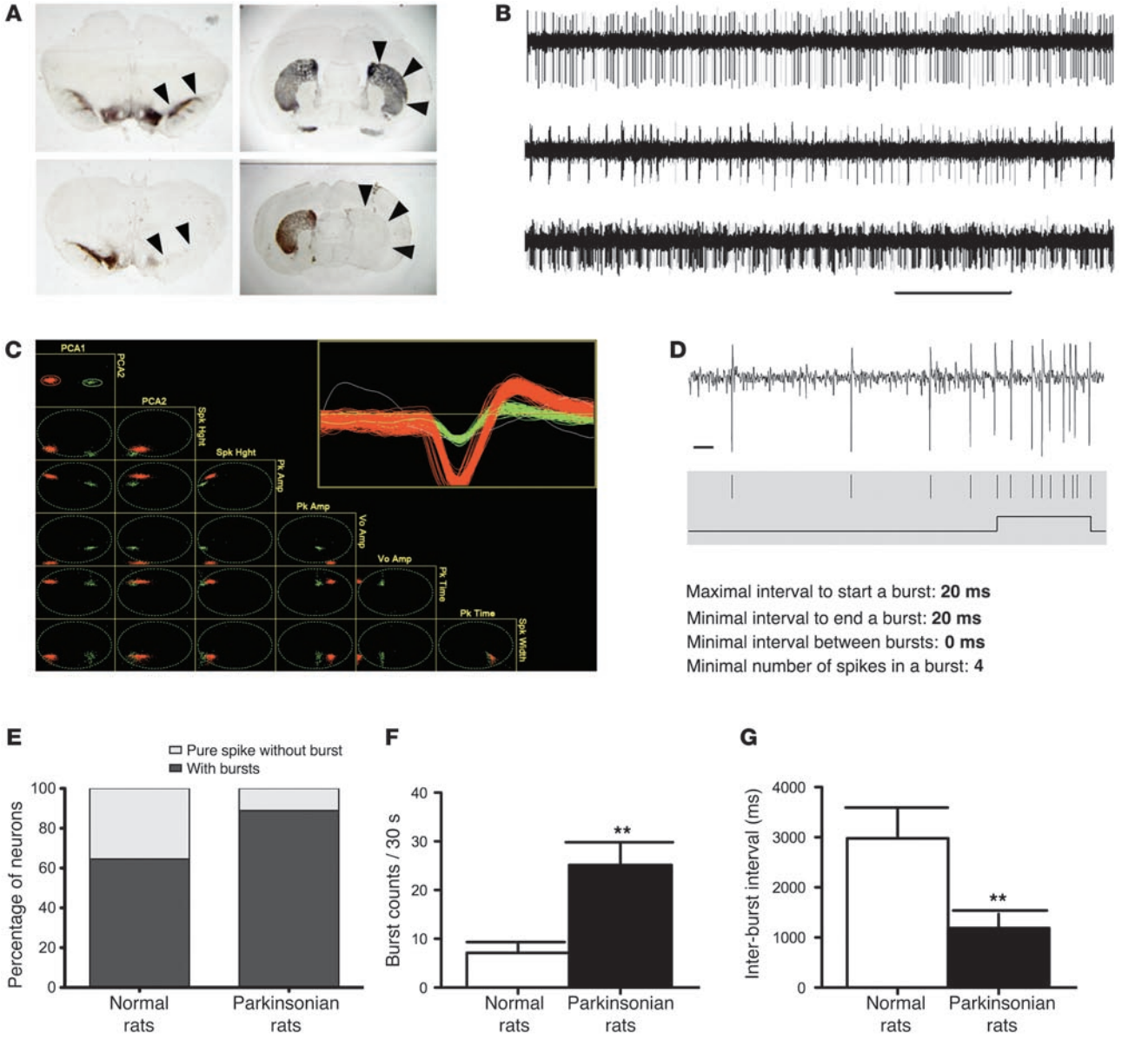

Figure 7

Increased in vivo burst discharges of STN in parkinsonian rats. In total, 26 single units of STN neurons were recorded in 3 normal rats, and 53 single units were recorded in 6 parkinsonian rats. (**A**) Tyrosine hydroxylase immunohistochemistry of brain sections from normal and parkinsonian rats. Note the severe loss of dopaminergic cells in the SNc (left panels, arrowheads) and the striatum (right panels, arrows) after unilateral lesion by 6-OHDA (lower panels) compared with the control group (upper panels). (**B**) Representative in vivo recordings from STN in parkinsonian rats showing spiking (tonic, upper trace), burst (phasic, middle trace), and mixed (lower trace) types of firing. (**C**) Detected spikes were sorted with the PCA algorithm. The inset shows the morphology of spikes in each selected single unit (red or green) and unselected spikes (white). (**D**) Burst detection parameters used for the single-unit spike trains. A trace of STN single-unit recording (top) with raster of sorted spikes (middle) and the result of burst detection (bottom) is shown as an example. See Methods for details. (**E**) There are more STN neurons firing in the burst mode in the parkinsonian rats (n = 53) than in the control group (n = 26). The percentage of neurons that are free of burst firing is markedly lower in the parkinsonian group (11.1%) than in the control (normal) group (35.5%). (**F**) The burst counts in the 30-second recording session increase significantly in the parkinsonian rats. (**G**) The inter-burst interval is significantly shortened in the parkinsonian rats. Scale bars: 2 seconds and 10 ms for **B** and **D**, respectively. $^{**}P < 0.01$, normal versus parkinsonian rats.

the tonic spiking discharges at the same concentrations (Figure 6C). All the actions of the pharmacological agents on subthalamic neuronal activities in brain slices thus are well in line with the view that inhibition of T-type Ca^{2+} channels leads to decreases in the burst discharges in STN.

Dopamine depletion causes increased in vivo burst discharges of STN in parkinsonian rats. To explore the pathophysiological implications of the findings from in vitro recordings, we further studied the in vivo discharge of STN and locomotor behavior in 6-hydroxydopamine–lesioned (6-OHDA–lesioned) parkinsonian rats (see Meth-

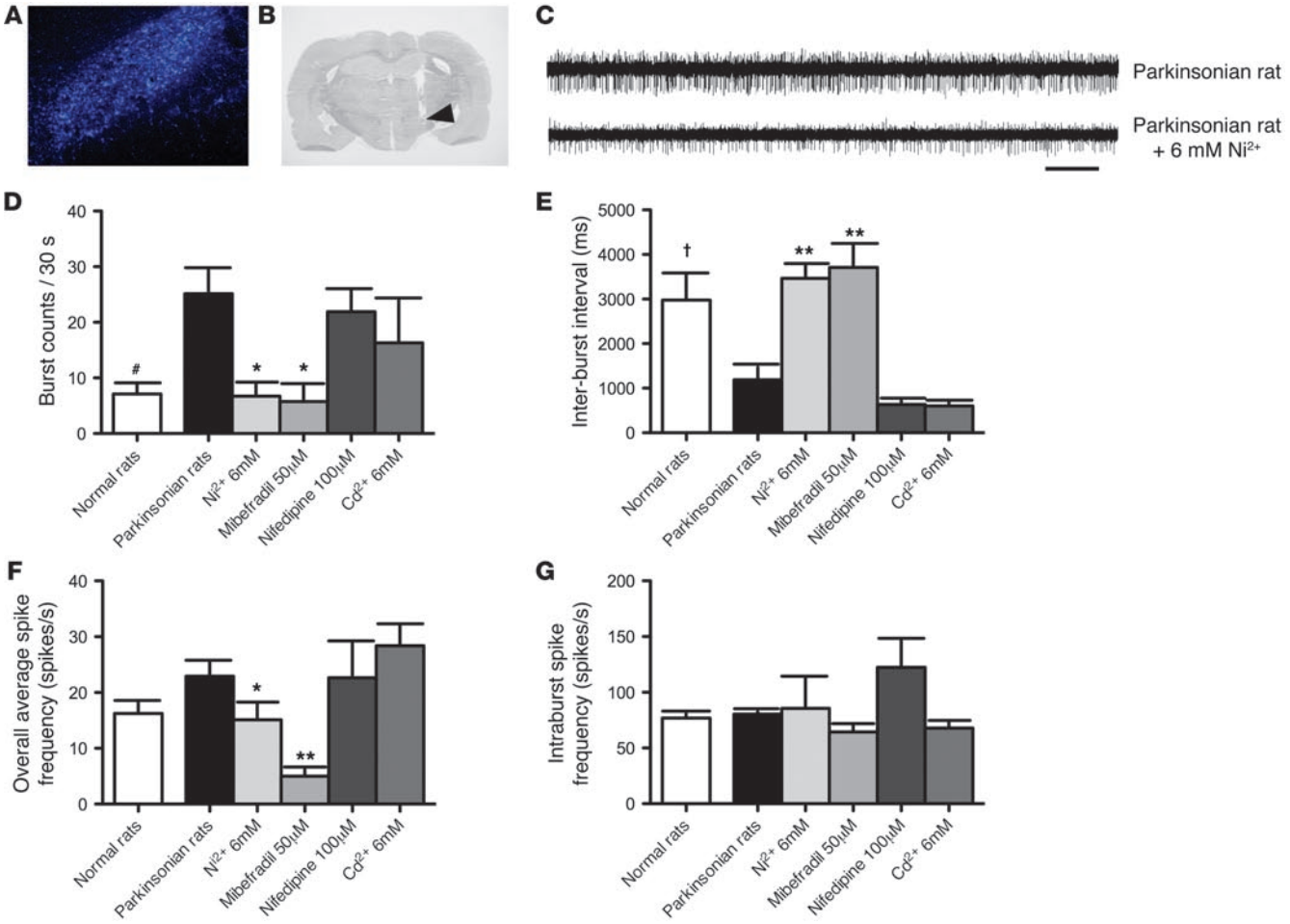

Figure 8

Decrease in in vivo burst discharges in parkinsonian rats by local administration of T-type Ca^{2+} channel blockers into STN. (**A**) The location of STN is confirmed by retrograde labeling of Fluoro-Gold injected into the globus pallidus (original magnification, ×80). (**B**) Verification of the location of the implanted cannula tip in STN (indicated by an arrow) of rat coronal brain section by cresyl violet staining. (**C**) Traces of in vivo single-unit recording of a STN neuron before and after microinjection of 6 mM Ni^{2+} into STN in a parkinsonian rat. Scale bar: 2 seconds. (**D**–**G**) The changes in different parameters of STN discharges in parkinsonian rats before (n = 53) and after administration of different Ca^{2+} channel blockers, including 6 mM Ni^{2+} (n = 11), 50 μM mibefradil (n = 9), 100 μM nifedipine (n = 7), and 6 mM Cd^{2+} (n = 9), are compared (*P < 0.05, **P < 0.01). Data of control (normal) and parkinsonian rats without drugs shown in **D** and **E** are taken from Figure 7 ($^{\#}P$ < 0.05 and $^{\dagger}P$ < 0.05, normal versus parkinsonian rats).

ods for the establishment of parkinsonian rats). Figure 7A shows tyrosine hydroxylase immunohistochemistry of brain sections from the parkinsonian rats to verify the success of the dopamine-depletion lesion in both the substantia nigra pars compacta (SNc) and the striatum. We then performed single-unit extracellular recording of subthalamic neurons in parkinsonian rats and isolated single units of neuronal firings in STN with spike sorting and analysis software (SciWorks version 5.0) (Figure 7, B–D; see Methods for details). Burst detection and quantification were performed according to the maximal interval method after single units were isolated and time stamps were digitized (Figure 7, C and D). Recordings of single-unit spike trains in STN revealed that there was a marked increase in both the number of neurons that fired in the burst mode and the burst count during a 30-second recording session, but a marked decrease in the inter-burst interval, in the parkinsonian rats (Figure 7, E–G). Both the burst duration (89.4 ± 7.1 vs. 57.4 ± 2.8 ms) and the number of spikes in each burst (7.4 ± 4.6 vs. 4.2 ± 0.7 ms) were also increased in the parkinsonian rats compared with the control group (data not shown). These data indicate a significant increase in the tendency of bursts in STN of parkinsonian rats.

Local administration of Ni^{2+} and mibefradil, but not nifedipine and Cd^{2+}, decreases in vivo burst activity of STN in parkinsonian rats. Our in vitro data showed that pharmacological inhibitors of T-type Ca^{2+} channels decrease the burst rates in STN slices. We then investigated their effects on in vivo subthalamic discharges in parkinsonian rats. The channel inhibitors were directly injected into STN via a chronically implanted intracranial stainless cannula, the location of whose tip was always verified histologically to be in the STN region after the experiments (Figure 8, A and B). As found in vitro, we found that microinjection of Ni^{2+} and mibefradil, two relatively specific blockers of T-channels (Figures 1 and 2), into STN significantly

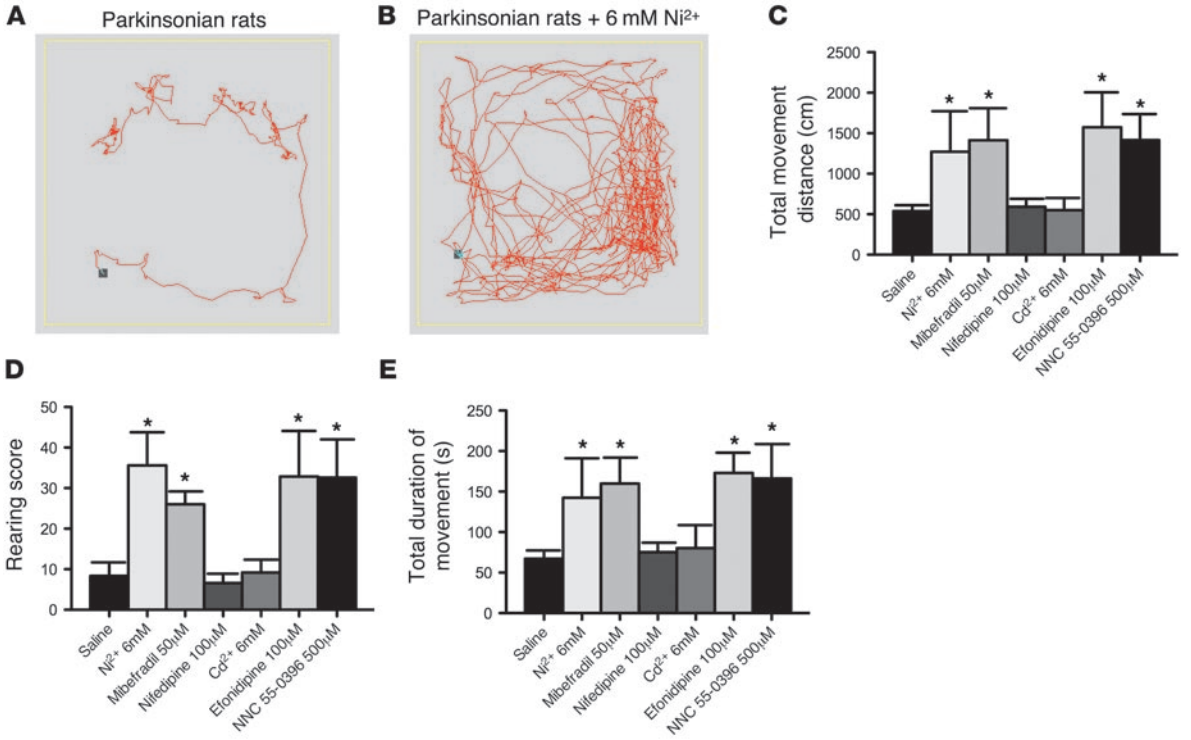

Figure 9
Remedy of locomotor deficits of parkinsonian rats by T-type Ca^{2+} channel blockers. (**A** and **B**) Sample plots of the locomotor traces of a parkinsonian rat in an arena with administration of normal saline (**A**) and 6 mM Ni^{2+} (**B**). Marked increase in the locomotor activities is apparent after administration of 6 mM Ni^{2+}. (**C**–**E**) The changes in total movement distance (**C**), rearing score (**D**), and total duration of movement (**E**) in the parkinsonian rats with intracranial injection of 6 mM Ni^{2+}, 50 μM mibefradil, 100 μM nifedipine, 6 mM Cd^{2+}, 100 μM efonidipine, or 500 μM NNC 55-0396 (each $n = 5$) are compared with those with intracranial injection of normal saline ($n = 20$) into STN (*$P < 0.05$).

decreased the burst rate (number of bursts in a 30-second recording session) and lengthened the inter-burst interval of STN neurons in the lesioned rats (Figure 8, C–E). A significant decrease in the number of spikes per burst after Ni^{2+} microinjection was also noted (7.1 ± 1.4 vs. 3.8 ± 0.2, $P < 0.05$, data not shown). In the presence of either Ni^{2+} (6 mM) or mibefradil (50 μM), both the burst rate and the inter-burst interval (and also the number of spikes per burst and the burst duration; data not shown) were "corrected" to the level of the control (normal) animals (Figure 8, D and E). In contrast, microinjection of either HVA Ca^{2+} channel blocker Cd^{2+} or specific L-type Ca^{2+} channel blocker nifedipine at high concentration failed to decrease the burst rate or increase the inter-burst interval in STN (Figure 8, D and E). Because extensive diffusion of injected drugs seemed to be unavoidable in this in vivo study, we consistently used concentrations of drugs approximately 10-fold or higher than those used in vitro, under the premise that the relationship between the in vivo and in vitro concentrations may not be the same for different drugs. In any case, Cd^{2+} and nifedipine, at concentrations at least 10-fold higher than the effective concentrations against L-type Ca^{2+} currents in vitro (see Figure 5), showed no significant effect on STN burst rates. In contrast, Ni^{2+} and mibefradil, at concentrations 10-fold higher than the effective concentrations against LVA Ca^{2+} currents in vitro, showed a prominent decrease in STN burst rates (see also the animal behavior data below). The other parameters of subthalamic discharges, such as the overall average firing frequency and the intra-burst spike frequency, which were not changed by the 6-OHDA lesion, also did not seem to be changed by Cd^{2+} or nifedipine (Figure 8, F and G). On the other hand, Ni^{2+} and mibefradil significantly decreased the overall average but not the intra-burst spike frequency. These findings suggest that the availability of T-type Ca^{2+} channels may play a fundamental role in the increased burst rates (and probably also other key electrophysiological features) of STN in vivo in parkinsonian rats.

T-type Ca^{2+} channel blockers remedy locomotor deficits in parkinsonian rats. In light of the findings that T-type Ca^{2+} channel inhibitors may reverse the effect of dopamine depletion on subthalamic discharge patterns, we further investigated whether modulation of T-type Ca^{2+} channels can actually alter the locomotor activity in parkinsonian rats. We performed an open field locomotor activity test (OFT) to examine spontaneous locomotor activity (see Methods for details). The parkinsonian rats show a marked decrease in the distance of horizontal movement, the number of rearings, and the total time of movement (see below). We did not observe obvious rotational behavior in the parkinsonian animals. The reliability of OFT was examined in a repeated test session. With two daily sessions of OFTs in 5 consecutive days, the responses in movement distance and duration were stable and reproducible. Each animal underwent two sessions of OFT during the experimental day, with normal saline directly injected into STN in the first session and with different Ca^{2+} channel inhibitors in the second session for comparison. We found that direct microinjection of either 6 mM Ni^{2+} or 50 μM mibefradil into STN markedly improved the locomotor activity of the parkinsonian rats for all parameters tested during the 5-minute test session, including total movement dis-

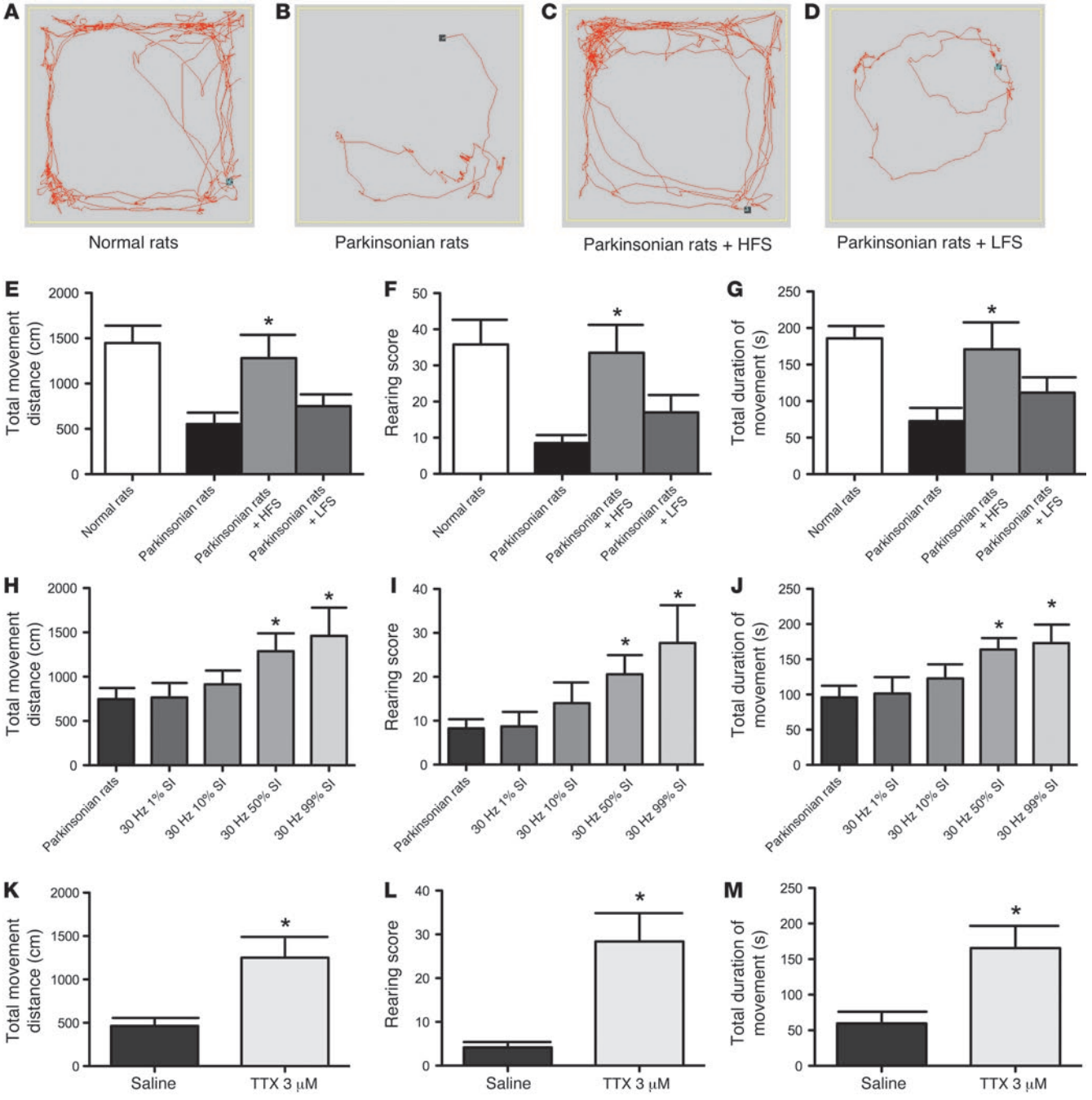

Figure 10

Parkinsonian locomotor deficits effectively treated by delivery of electrical current with adequate depolarization of STN neurons. (**A**–**D**) Plots of the locomotor traces of control (**A**) and parkinsonian (**B**) rats and of parkinsonian rats receiving high-frequency stimulation (HFS) at 130 Hz (**C**) and low-frequency stimulation (LFS) at 30 Hz (**D**). (**E**–**G**) Different parameters of locomotor activities in normal and parkinsonian rats with and without HFS or LFS. The group of parkinsonian rats with HFS or that with LFS is compared with the control parkinsonian group ($n = 6$ for each group, $^*P < 0.05$). (**H**–**J**) Administration of 30 Hz negative current stimulation with different pulse widths (1% SI = 333 μs, 10% SI = 3,333 μs, 50% SI = 16,667 μs, 99% SI = 33,000 μs). Significant improvement in locomotor parameters is obtained with 50% SI and 99% SI. $n = 7$; $^*P < 0.05$, compared with sham stimulation. (**K**–**M**), Topical administration of 3 μM TTX into STN can also remedy locomotor deficits in parkinsonian rats ($n = 5$; $^*P < 0.05$, rats with versus without TTX administration).

tance, rearing score, and total duration of movement (Figure 9). Actually, even at low concentrations, Ni^{2+} (e.g., 0.6 mM, as used in in vitro studies) led to a clear trend toward improvement in all locomotor parameters tested (our unpublished observations). In contrast, locomotor activity was not significantly improved after local administration of 100 μM nifedipine or 6 mM Cd^{2+} into STN. To further specify the target underlying the behavioral effect of Ni^{2+} and mibefradil, we also demonstrated a similar beneficial effect

on locomotor activities with 500 μM NNC 55-0396 and 100 μM efonidipine (Figure 9, C–E). The remarkably similar effect of efonidipine serves to argue against the possibility that the remedying effect of Ni^{2+}, mibefradil, and NNC 55-0396 arises from their action on the other nonspecific conductances, whereas the lack of effect of Cd^{2+} and nifedipine would argue against the conclusion that the effect of efonidipine arises from the inhibition of L-type Ca^{2+} channels. We have also examined the effect of infusion of 6 mM Ni^{2+}, 50 μM mibefradil, or 100 μM efonidipine into STN and found no significant effect on locomotor behavior in normal rats (our unpublished observations). The effects of Ni^{2+}, mibefradil, and efonidipine thus are unlikely ascribable to any nonspecific hyperkinetic effect. These data together argue strongly for an essential role of T-type Ca^{2+} channels in parkinsonian motor deficits. It is plausible that inhibition of T-type Ca^{2+} channels would reduce subthalamic burst discharges and thus effectively remedy the locomotor deficits of parkinsonian rats.

30-Hz stimulation with a longer depolarizing pulse also remedies locomotor deficits in parkinsonian rats. To further examine the similarity between the rat model and the clinical conditions of PD, we also delivered high- or low-frequency stimulation of STN through a chronically implanted stimulating electrode ipsilateral to the lesion side. During high-frequency stimulation at 130 Hz, we found that there was dramatic amelioration of the locomotor deficits in total movement distance, rearing score, and total movement duration, making the locomotor behaviors of the parkinsonian rats nearly comparable to those of normal rats. In contrast, low-frequency stimulation at 30 Hz was much less effective (Figure 10, B–G). The results demonstrate that the animal model is apparently very much consistent with the clinical electrophysiological and behavioral findings in PD. In light of our findings that the availability of T-type Ca^{2+} currents could be critically involved in the pathogenesis of parkinsonian locomotor deficits, we wondered whether it is the overall duration of depolarization (for the inactivation of enough T-channels) rather than specific frequency of current injection that makes DBS at 130 Hz much more effective than DBS at 30 Hz. We thus lengthened the duration of each stimulation pulse but kept the stimulation frequency at 30 Hz. Instead of the regular 60-μs pulse width, we administered 30-Hz negative current stimulation into STN of parkinsonian rats with increasing pulse widths of 333 μs, 3,333 μs, 16,667 μs, and 33,000 μs (1%, 10%, 50%, and 99% stimulus interval [SI], respectively). We found that the locomotor deficits of the parkinsonian rats could be rescued after they received 30 Hz stimulation with longer stimulation pulse width (Figure 10, H–J). Total movement distance, rearing score, and total duration of movement in parkinsonian rats all gradually increased with the length of depolarizing pulse width (Figure 10, H–J). We also applied 15 Hz stimulation, and found very similar effect (1% SI was ineffective, whereas 50% and 99% were effective; our unpublished observations). The critical parameter of DBS therapy thus may be not the stimulation frequency, but the amount of charge delivered to depolarize the cell membrane and consequently inactivate relevant ion channels (see Discussion). In summary, either electrophysiological maneuvers or pharmacological agents that decrease the availability of T-channels and the burst rates in STN would presumably substantially ameliorate locomotor deficits in PD. To further substantiate the therapeutic role of decreased burst discharges in parkinsonian rats, we also applied tetrodotoxin (TTX) to inhibit Na^+-mediated spikes. Administration of 3 μM TTX into STN essentially abolished all firing activities, whether burst or tonic (data not shown) and also significantly improved all parameters of locomotion in the parkinsonian rats (Figure 10, K–M). We already noted that dopamine depletion caused an abnormal STN discharge pattern characterized by increased burst discharges and decreased spiking discharges. This finding with TTX would further support the essential role of increased burst rather than decreased spiking discharges of STN in the genesis of parkinsonian locomotor deficits.

Discussion

The causal relationship between increased STN burst discharges and the genesis of locomotor deficits in PD. Clinical findings have shown that typical PD symptoms such as rigidity, bradykinesia, and tremor may be associated with pathologically enhanced oscillations in the basal ganglia (as well as its interconnected units in the functional networks such as sensorimotor cortex and ventrolateral thalamus) (44–50). In experimental models, an increase in subthalamic bursts has also been found with MPTP- or 6-OHDA–induced parkinsonian states (51). However, the causal role of the increased burst discharges in parkinsonian motor deficits has yet to be clarified. Here we found that electrophysiological maneuvers or pharmacological agents that decrease bursts readily remedy the locomotor deficits in parkinsonian animals, whereas those that do not reduce bursts show little effect on locomotor deficits. Most interestingly, efonidipine — which did not significantly affect spontaneous tonic spiking discharges but turned burst into spiking patterns of firing — also showed a significant improvement in locomotor parameters. In other words, the data suggest that if the level of burst activity in STN is low enough, there will be no significant parkinsonian locomotor deficits. Our findings thus provide the first demonstration to our knowledge that increased burst discharges in STN make an essential contribution to, or even are the direct cause of, the locomotor deficits in the parkinsonian state. Physiologically speaking, an increase in burst discharges may increase the chance of the postsynaptic neurons to follow the activity of the presynaptic neuron, and thus result in more synchronized oscillatory discharges in the circuits. In this regard, we have noted that, along with increased burst discharges, the prevalence of silent STN neurons seemed to also increase with 6-OHDA lesion. Whether these silent STN neurons contribute to PD is unknown. However, their role may not be as significant as that of increased bursts considering that complete silencing of STN neurons by either local application of TTX to STN (Figure 10, K–M) or surgical subthalamotomy (52) may also alleviate parkinsonian locomotor symptoms. We would therefore propose that at least part of the burst discharge pattern should be necessary to drive the basal ganglia circuits into a definite pathological state (in which the circuits may no longer appropriately transform and relay the initial motor commands from the cerebral cortex) and that any maneuver capable of disrupting the genesis of such burst discharges would potentially ameliorate or even abolish the motor symptoms of PD.

The critical role of T-type Ca^{2+} channels in the genesis of STN burst discharges. The ionic mechanisms underlying the spontaneous single spikes in STN have been related to resurgent or persistent Na^+ channels and apamin-sensitive Ca^{2+}-dependent K^+ conductance (16–18). However, the ionic mechanisms of bursting activity in STN have been far less well characterized (27). Both extracellular single-unit recording in vivo and cell-attached recording in STN slices showed a robust decrease in burst discharges of STN neurons with different T-type Ca^{2+} channel inhibitors (Figures 4, 6,

and 8). These findings indicate that ionic mechanisms underlying subthalamic bursts have to involve T-channels. The involvement of T-type Ca^{2+} conductance is further supported by the whole-cell recording of acutely dissociated STN neurons, where electrophysiological and pharmacological characterizations suggest possible involvement of Ca_v 3.1 channels, consistent with the findings based on Northern blot analysis in human STN (53). Nakanishi et al. showed that TTX-resistant but Co^{2+}-sensitive slow action potentials are triggered by hyperpolarization of the membrane to more negative than –65 mV and may subsequently induce a burst of firing in STN neurons (19). In this regard, our data would indicate that sufficient T current probably is necessary to drive burst discharges from a more negative resting membrane potential. Nevertheless, some T-currents may also be involved in the genesis of single-spike discharges (Figure 4). The relatively slow inactivation kinetics of T-channels compared with the duration of each action potential spike suggests the requirement of a few densely packed spikes to inactivate T-channels, constituting a possible factor that determines the length of a burst. Taken together, our findings indicate that T-channel blockers may assume a novel and effective role in the symptomatic treatment of PD (also see below).

Possible origin of the differential effects between high- and low-frequency stimulation of STN in the treatment of PD. Delivery of electrical current into STN has been used as a standard treatment modality for PD. Although high-frequency (e.g., >90 Hz) stimulation of STN improves motor symptoms in PD patients, low-frequency (e.g., 20–30 Hz) stimulation is relatively ineffective, or could even worsen the clinical symptoms (15). These intriguing observations have puzzled clinical electrophysiologists and neurologists for a long time, but can now be understood in light of the causal role of T-type Ca^{2+} channels and burst discharges of subthalamic neurons in parkinsonian symptoms. Single-spike discharges of STN faithfully relaying the motor commands from the motor cortex are favored by a relatively depolarized resting membrane potential of the subthalamic neuron. When the resting membrane potential is mildly to moderately hyperpolarized, burst discharges become more prevalent (27). In this case, the cortical input may be less faithfully followed by the STN neuronal response, probably because the input may not be strong enough to drive the membrane potential to the threshold of action potential generation, and the subthalamic neuron tends to fire in autonomous or even semi-periodic bursts whenever enough T-channels are revived from inactivation by the relatively negative membrane potential. However, if the membrane potential becomes profoundly hyperpolarized, even burst discharges cannot occur because the threshold of an action potential is hardly reached even when most T-channels are open. In this regard, low-frequency stimulation, which represents a weaker depolarizing force than high-frequency stimulation, may sometimes bring the membrane from profoundly to moderately hyperpolarized and thus increase the tendency of burst discharges. High-frequency stimulation, on the other hand, tends to bring the membrane to a more depolarized level and thus decrease the tendency of burst discharges. Moreover, T-channels in the thalamus recover with an initial delay of approximately 13.5 ms at –100 mV (and this delay could be >20 ms at more depolarized recovery potentials), followed by an exponential phase characterized by a time constant as slow as approximately 300 ms at approximately 25°C (54). Although the kinetics could all be faster in vivo (37°C), it is quite conceivable that high-frequency stimulation at approximately 130 Hz will be much more effective than low-frequency stimulation at approximately 30 Hz in decreasing the available T-type Ca^{2+} channels to a critical level, no longer capable of initiating and/or sustaining burst discharges. This idea was substantiated by the amelioration of locomotor symptoms by 30-Hz stimulation with longer depolarizing pulse (Figure 10, H–J), and provides a good explanation for the recent finding that DBS does not silence but rather shifts firing of STN neurons toward a more random pattern (55). Together with the findings that T-type Ca^{2+} channel inhibitors also show a similar beneficial effect, inactivation of T-type Ca^{2+} channels is very likely involved in the molecular mechanism underlying the therapeutic effect of DBS. The delivered charges and altered membrane potential may also have an effect on the availability of Na^+ channels (17). The effectiveness of the modified 30 Hz DBS (Figure 10, H–J) could thus be ascribable to inactivation of the T-type Ca^{2+} and/or Na^+ channels. In any case, the altered channel availability is probably an important molecular substrate underlying DBS therapy. It is possible, then, that the electrophysiological modulation of STN via DBS can be adjusted with a more rational basis to improve the efficacy of PD therapy.

Physiological and clinical implications. It is noteworthy that decreased burst discharge of STN or even silenced STN (by TTX or local lesions) may be beneficial for the PD patient in terms of all major categories of symptoms, including rigidity, bradykinesia, and tremor (52, 56). This observation seems to imply that the major symptoms of PD actually are ascribable to a gain rather than a loss of function in the motor circuits. The STN probably is not essential for the genesis of basic motor engrams but may exert a strong modulatory effect on the proper execution of the engrams. Specifically, for the execution of each motor engram originating from the motor cortex, the hyperdirect pathway directly connecting cortex to STN very likely introduces the first incoming volleys to reach the internal segment of the globus pallidus and the substantia nigra pars reticulata (Gpi/SNr). Nambu (57) postulated that this hyperdirect pathway would clear the previous engrams and set a clean stage for the execution of the current engram. However, the hypothetical function seems to be somewhat redundant if one agrees that the indirect pathway also serves to clear the engrams executed by the direct pathway. We would propose that the hyperdirect pathway, the first message to come back to the thalamocortical network after the impulse formation in the motor cortex and travel through the basal ganglion loops, might be more appropriately viewed as an active feed-forward modulatory mechanism related to the fine-tuning of the current engrams rather than a feedback inhibitory mechanism cleaning up the executed engrams. In other words, when a motor engram is initially formed in the thalamocortical network, it is sent through the hyperdirect pathway to determine its details in speed and dimension (to filter the intrinsic noises that may be associated with the signal). Thus, the most common motor symptom associated with acute lesions of STN is hemiballism, a disordered limb movement characterized by erroneous speed and dimension, and most importantly, a disordered limb movement showing a strong tendency to occur when the patient is having an intention (even just a very slight intention) to move the affected limbs. The rigidity, bradykinesia, and even tremor in PD patients thus may be caused by the inappropriate bursting impulses feeding into the thalamocortical network via Gpi/SNr from STN. This may also be the reason why the patients of PD may have a significant symptomatic improvement with the decrease of the aforementioned bursts by high-frequency DBS. However, these patients would usually have persistent problems

in the execution of motor tasks where high speed and accurate dimension are required, because the high-frequency stimulation itself may cause some deranged impulses from STN. With the identification of the key role of T-type Ca^{2+} channels and burst discharges of STN in parkinsonian symptoms, it would be interesting to explore the effect of different channel blockers or modulators, alone or in combination with one another or with electrophysiological stimulation, on the locomotor deficits in PD in a more rational way. This study thus indicates possible novel avenues for the mechanistic understanding and treatment of PD.

Methods

Brain slice preparation and extracellular recordings. All experiments were approved by the of Institutional Animal Care and Use Committees of National Taiwan University College of Medicine and College of Public Health and of Chang Gung University. We first performed in vitro extracellular recordings in brain slices obtained from C57BL/6 mice (aged p16–p32). Experiments were repeated with control (normal) and parkinsonian Wistar rat brain slices to check for consistency. The whole brain was rapidly removed under isoflurane anesthesia and immersed into ice-cold oxygenated cutting solution (containing [in mM] 87 NaCl, 37.5 choline chloride, 25 $NaHCO_3$, 25 glucose, 2.5 KCl, 1.25 NaH_2PO_4, 7 $MgCl_2$, and 0.5 $CaCl_2$). A parasagittal brain slice (250 μm thick) that contained the STN was then cut on a vibratome (Leica VT1000S). The slice was incubated in the oxygenated cutting solution for 25 minutes at 30°C and then transferred into oxygenated saline for 25 minutes at 30°C before electrophysiological recording. The saline contained (in mM) 125 NaCl, 26 $NaHCO_3$, 25 glucose, 2.5 KCl, 1.25 NaH_2PO_4, 1 $MgCl_2$, and 2 $CaCl_2$. The STN was identified with a low-power (×4) objective, and individual neurons were visualized with a ×60 water immersion objective on an upright microscope (BX51WI, Olympus). The loose-seal cell-attached current-clamp recording was performed at room temperature with 3–6 MΩ pipettes filled with 0.9% NaCl- or K^+-based solution (in mM, 116 $KMeSO_4$, 6 KCl, 2 NaCl, 20 HEPES, 0.5 EGTA, 4 MgATP, 0.3 NaGTP, 10 $NaPO_4$ creatine, and pH 7.25 adjusted with KOH). Firing activities were not different when 0.9% NaCl- or K^+-based solution was used as the pipette solution. Cells were recorded in the current-clamp mode. Recordings were acquired with a Multiclamp 700B amplifier (MDS Analytical Technologies), filtered at 5 kHz, and digitized at 10–20 kHz with a Digidata-1440 analog/digital interface along with pCLAMP software (MDS Analytical Technologies). Data were also analyzed using pCLAMP. Burst detection and analysis were performed according to the maximal interval method with the same criteria as those described in in vivo electrophysiological data analyses below. Pharmacological agents were dissolved in DMSO or distilled water, stored at –20°C, and diluted 1:1,000 into the bath reservoir to reach the experimental concentrations immediately before application. Bath application of 1:1,000 DMSO did not significantly alter any response under investigation. Constant bath flow was ensured by a perfusion pump (Gilson Medical Electric) at a flow rate of 5 ml/min, and the dead space in the perfusion tubing was reduced to 1 ml, allowing stable and rapid bath exchange of pharmacological agents.

Preparation of acutely dissociated STN neurons. For the preparation of acutely dissociated STN neurons, we first obtained brain slices from Wistar rats aged p8–p18 with procedures similar to those described above, except that 400-μm-thick slices were cut. Parasagittal slices containing STN were then incubated in the oxygenated cutting solution at 33°C for 15 minutes. After treatment for 2–5 minutes at 33°C in the oxygenated cutting solution containing 1 mg/ml protease XXIII (Sigma-Aldrich), the slices were thoroughly washed by the cutting solution containing 1 mg/ml bovine serum albumin (Sigma-Aldrich) and then incubated in the oxygenated cutting solution at room temperature. Immediately before use, the STN chunk was removed to dissociation medium (in mM, 82 Na_2SO_4, 30 K_2SO_4, 3 $MgCl_2$, and 5 HEPES, pH 7.4) and triturated with a fire-polished Pasteur pipette to release single neurons.

Electrophysiological recordings in acutely dissociated neurons. The dissociated STN neurons were put in a recording chamber containing Tyrode's solution (in mM, 150 NaCl, 4 KCl, 2 $MgCl_2$, 2 $CaCl_2$, and 10 HEPES, pH 7.4). Whole-cell voltage clamp recordings were obtained at room temperature using approximately 1.0 MΩ borosilicate micropipettes (Hilgenberg Inc.) filled with the appropriate internal solution. The standard internal solution was (in mM) 121.5 NMDG-phosphate, 9 EGTA, 9 HEPES, 1.8 $MgCl_2$, 4 MgATP, 0.3 GTP-Tris, 14 phosphocreatine (Tris salt), pH 7.4. The internal solution especially designated for recording of chiefly T-type Ca^{2+} channel currents contained (in mM) 100 NMGF, 50 NMGCl, 5 mM EGTA, 3 $MgCl_2$, and 10 HEPES (pH 7.4). The intracellular fluoride ion was used to facilitate the run-down of the L-type Ca^{2+} channel current (58, 59). A seal was formed and the whole-cell configuration obtained in Tyrode's solution. The cell was then lifted from the bottom of the chamber and moved in front of an array of flow pipes (Microcapillary from Hilgenberg Inc.; content 1 μl, length 64 mm), which, unless otherwise specified, emitted the TEA-based Na^+-free external recording solutions (in mM, 150 TEACl, 5 $CaCl_2$, 10 HEPES, and pH 7.4 adjusted with TEAOH) in the absence or presence of different channel blockers or modifiers [e.g., Ni^{2+}, Cd^{2+}, mibefradil, NNC 55-0396 ([1S,2S]-2-(2-(*N*-[(3-benzimidazol-2-yl)propyl]-*N*-methylamino)ethyl)-6-fluoro-1,2,3,4-tetrahydro-1-isopropyl-2-naphtyl cyclopropanecarboxylate dihydrochloride], nifedipine, and efonidipine]. For recording of subthalamic Na^+ currents in Figure 2B and Figure 6C, the external solution was replaced by a low-calcium Tyrode's solution that contained (in mM) 150 NaCl, 4 KCl, 5 $MgCl_2$, 0.3 $CaCl_2$, 0.3 $CdCl_2$, and 10 HEPES, pH 7.4. The cell was moved between the control and the drug-containing external solution. When the cell was moved into any solution, we always waited until the currents were stable for at least 5 sweeps. The effect of the drug was then calculated according to the level of the stable currents. Recordings were acquired with a Multiclamp 700B amplifier (MDS Analytical Technologies), filtered at 5 kHz, and digitized at 20–50 kHz with a Digidata-1440 analog/digital interface along with pCLAMP software (MDS Analytical Technologies).

6-OHDA injection and animal model of parkinsonism. In vivo experiments were carried out on adult male Wistar rats weighing 260–400 g. Animals were housed at constant temperature and humidity under a 12-hour light/12-hour dark cycle with free access to food and water. We made unilateral 6-OHDA (Sigma-Aldrich) lesions to establish a rat model of parkinsonism. The extent of dopamine depletion in the basal ganglia circuitry was verified by the nearly complete loss of tyrosine hydroxylase reactivity in the ipsilateral striatum and substantia nigra (Figure 7A). Five milligrams of 6-OHDA was dissolved in 2.5 ml of 0.9% normal saline (containing 0.01% ascorbic acid) and stored in the dark at 4°C before use. Rats were anesthetized with chloral hydrate (400 mg/kg, i.p.) (Sigma-Aldrich), mounted in a stereotactic frame (Narishige) and pretreated with desipramine hydrochloride (25 mg/kg, i.p.) (Sigma-Aldrich) to protect noradrenergic neurons. After a 30-minute interval, a hole was drilled above the substantia nigra, and a stainless steel cannula connected by a polyethylene catheter to a Hamilton microsyringe driven by an infusion pump (Harvard Apparatus) was inserted according to coordinates of substantia nigra pars compacta (SNc) indicated in the atlas (60): AP –5.0, L 2.2, D 7.5. A total volume of 4 μl of the foregoing 6-OHDA solution was then infused over a period of 8 minutes. The cannula was then left in place for 10 minutes before being slowly withdrawn. Seven to 10 days after surgery, the rats were tested for rotational behavior under subcutaneous injection of apomorphine (0.05 mg/kg, s.c.). Only rats with prominent turning behavior (more than 25

turns in 5 minutes) toward the side contralateral to the lesion side were considered as having severe dopaminergic depletion and designated as the parkinsonian rats, and these were retained for further electrophysiological and behavioral studies 2–4 weeks later.

Tyrosine hydroxylase immunohistochemistry. Lesions of dopaminergic neurons were confirmed by tyrosine hydroxylase immunohistochemistry. Serial sections of the substantia nigra and the striatum were processed for free-floating tyrosine hydroxylase immunohistochemistry. Sections were preincubated with 3% normal horse serum in TBS containing 0.3% Triton X-100 (TBST, Sigma-Aldrich) for 30 minutes at room temperature and then incubated in TBST containing 1% normal horse serum and monoclonal antibody to tyrosine hydroxylase (Sigma-Aldrich) for 24 hours at 4°C. After washing in TBST, the brain sections were incubated with biotinylated anti-mouse IgG for 2 hours at room temperature. Sections were rinsed again in TBST containing 1% normal horse serum and incubated with ExtrAvidin peroxidase (1:500, Sigma-Aldrich) for 1 hour at room temperature. Sections were then exposed to a mixture of 3,3′-diaminobenzidine, H_2O_2, and Ni^{2+} (DBA kits; Vector Laboratories). Sections were fixed on gelatin-coated slides, dehydrated with alcohol in ascending concentrations, cleaned in xylene, mounted by Permount (Fisher Scientific), and then covered with cover glass.

Implantation of the stimulation electrode and the microinjection cannula for chronic use. Under chloral hydrate anesthesia, the rat was placed in a stereotaxic instrument. After an adequate sterilization procedure, the skull was exposed and a hole was drilled unilaterally through the skull targeting the STN region in a plane 90° to the horizontal line and parallel to the sagittal plane. A plastic cylindrical rod holding a stainless steel cannula or a cannula with stimulation electrode (PlasticsOne) was centered on the hole. The tip of the cannula was inserted according to the stereotaxic coordinate of STN (AP 3.8 mm, L 2.4 mm, D 7.5 mm from bregma) and was lowered to the level of the upper part of STN. The plastic rod was then secured with dental cement attached to 3 stainless steel screws drilled into the skull, and the scalp wound was then closed. The motor behavior and electrophysiological studies were performed 2 weeks after the implantation surgery.

Electrical stimulation and microinjection of different pharmacological agents into STN. A microinjection cannula or a stimulation metal microelectrode was lowered into STN during the electrophysiological studies according to the coordinates provided above but at an angle of 20° to the sagittal plane. A stainless steel cannula was connected to the microinjection syringe on a pump via polyethylene tubing and was used for microinjection of different pharmacological agents into STN. The rate of injection was 0.2 μl/min. The stimulation metal electrode was connected to an isolated stimulator (World Precision Instruments) under the command of a programmable stimulator (S3600, World Precision Instruments).

In vivo single-unit extracellular recording. Single-barrel glass micropipettes with microfilament were pulled into a microelectrode with tip diameter between 1 and 3 μm and impedance between 5 and 10 MΩ when filled with 3 M NaCl and 1% Chicago Sky Blue dye. The electrode was used for both single-unit recording and iontophoresis of pharmacological agents. The micropipette was placed above the center of a hole drilled on the coordinate of the STN (AP 3.8 mm, L 2.4 mm) and was advanced 6.5 mm below the skull surface near the dorsal border of the STN, which served as the starting point for single-unit recording. Electrophysiological signal was then amplified, filtered, converted through a digital-analog interface PowerLab 4SP (ADInstruments), and stored on a computer. Spike activity was also displayed on an oscilloscope. The search for unit activity began within 1 hour after electrode insertion and continued for 4–8 hours. After isolation of single-unit discharges (the signal-to-noise ratio set at 3:1 or higher), data collection typically lasted 5–10 minutes. After completion of the last recording session, rats were deeply anesthetized with urethane. Negative currents were then given through the micropipette, with the last site of recording/iontophoresis marked with pontamine sky blue dye. The rat was subsequently perfused transcardially with saline followed by 10% formalin. The brain was removed and stored for subsequent histological processing.

Histological verification of the location of STN and the implanted cannula. We identified the site of recording by retrograde labeling of STN neurons on the brain sections after electrophysiological recordings. After anesthesia with 4% chloral hydrate (0.8 ml/100 g body weight), a fluorescent dye, Fluoro-Gold (Fluorochrome; 2% in saline, 0.5 μl) was injected into the globus pallidus (AP –0.2, L 2.4, D 5.8) ipsilateral to lesion side. One week later, the rat was perfused transcardially, and the brain sections containing STN were obtained. Retrograde labeling was examined under an epifluorescence microscope (Olympus) to confirm the location of STN neurons (Figure 8A). In addition, hematoxylin staining was used to determine the location of microinjection of pharmacological agent into STN (i.e., the location of the chronically implanted microinjection cannula in STN; Figure 8B). Data were collected only from animals with a confirmed location of the cannula.

In vivo electrophysiological data analysis. The electrophysiological data were post-processed with spike detection and sorting tools from DataWave Technologies (SciWorks 5.0). Each spike was detected by threshold algorithm of its negative peak. The detected spikes were further sorted under the principal component analysis (PCA) algorithm. To ensure the quality of each sorted single unit, we used two objective and independent criteria for quantification. First, any unit whose signal-to-noise ratio was less then 3 was excluded from further analysis. Second, we examined the coefficient of variation (CV) over each of 5 spike profiles, including peak amplitudes, volley amplitudes, peak time, spike height, and spike widths in a single unit (see Figure 7C). Since each of these profiles should be clustered together for a true single unit, we exclude the signal units whose CV exceeded 0.9 in any of the 5 profiles. The sorted single units were further categorized to spiking or burst discharges according to their firing pattern. After a detailed examination of the differences in STN neuronal activity between normal and parkinsonian rat groups, the bursts were defined by the following parameters of interval algorithm: maximal interval to start a burst: 20 ms; minimal interval to end a burst: 20 ms; minimal interval between bursts: 0 ms; minimal number of spikes in a burst: 4 (Figure 7D). We analyzed the firing profiles including burst rates, inter-burst intervals, intra-burst spike frequencies, number of spikes in each burst, and burst duration in each single unit, and compared these profiles before and after the application of different ion channel blockers.

OFT. On the day of motor behavior tests, rats were transferred to a quiet, sound-attenuated behavior testing room at least 2 hours before the test session. The square arena (45 cm × 45 cm) was made of Plexiglas and equipped with a video recording and tracking system (EthoVision 3.0, Noldus) above the arena. The animals were first connected to the microinjection system by insertion of an inner injection cannula, which was connected to a microsyringe and a microinjection pump with polyethylene tubing. The pharmacological agent was administrated by an electrical microsyringe pump (Harvard Apparatus), with the speed set at 0.5 μl/min. Three minutes after the start of microinjection, the animal was placed in the center of the testing arena, and its locomotor behaviors were recorded with the video tracking system and saved in the hard disc of a personal computer for off-line analysis. For examination of the effect of high- or low-frequency stimulation of STN, the parkinsonian rats were tested for different behavior parameters. The same group of rats were subjected to two phases of testing. Each phase was performed on a separate day and included two 5-minute sessions. In the first phase of the study, the rats received sham stimulation (stimulus intensity: 0 μA; frequency: 130 Hz; duration of each stimulus: 60 μs) in the first session, and in the following session, unipolar high-frequency stimulation (stimulus

intensity: 300 μA; frequency: 130 Hz; duration of each stimulus: 60 μs) was administered 3 minutes before and during the 5-minute test session. In the second phase of the study, the same group of rats received low-frequency stimulation (stimulus intensity: 300 μA; frequency: 30 Hz; duration of each stimulus: 60 μs). When there was abnormal turning of the head or involuntary paw movement contralateral to stimulation, the stimulation intensity (300 μA as the initial setting) was lowered until disappearance of these dyskinetic movements. During sham stimulation, the parkinsonian rats all showed locomotor behaviors similar to those before any stimulation.

Statistics. In vivo numerical data and statistical analyses were managed with Prism software (GraphPad Software). Analyses of in vitro data, statistical tests, and curve fittings were performed using pCLAMP (MDS Analytical Technologies), SigmaPlot (Systat), and Excel (Microsoft) software. The data in Figures 3, 4, 7, and 10, K–M, were compared using unpaired (2-tailed) Student *t* tests, whereas the data in Figures 8, 9, and 10, A–J, were compared with 1-way ANOVA followed by Dunnett's test. All data are presented as mean ± SEM. For all comparisons, a *P* value less than 0.05 was accepted as indicative of significant differences.

Acknowledgments

We thank Wei-Hsin Yang and Janice Janing Lin for technical assistance. This work was supported by the National Science Council, Taiwan, grants NSC98-2321-B-002-012 (to C.-C. Kuo), NSC95-2314-B-002-082-MY3 (to C.-H. Tai), NSC97-2311-B-182-005-MY2 (to Y.-C. Yang), and NSC99-2311-B-182-001-MY3 (to Y.-C. Yang); by the National Health Research Institutes, Taiwan, grant NHRI-EX100-10006NI (to C.-C. Kuo); and by the Chang Gung Hospital, Taiwan, Medical Research Project CMRPD170453 (to Y.-C. Yang).

Received for publication January 20, 2011, and accepted in revised form May 11, 2011.

Address correspondence to: Chung-Chin Kuo, Department of Physiology, National Taiwan University College of Medicine, No. 1, Jen-Ai Rd., 1st Section, Taipei 100, Taiwan. Phone: 886.2.23123456, ext. 88236; Fax: 886.2.23964350; E-mail: chungchinkuo@ntu.edu.tw.

1. Alexander GE, Crutcher MD, DeLong MR. Basal ganglia-thalamocortical circuits: parallel substrates for motor, oculomotor, "prefrontal" and "limbic" functions. *Prog Brain Res*. 1990;85:119–146.
2. DeLong MR, Wichmann T. Circuits and circuit disorders of the basal ganglia. *Arch Neurol*. 2007;64(1):20–24.
3. Bergman H, Wichmann T, Karmon B, DeLong MR. The primate subthalamic nucleus. II. Neuronal activity in the MPTP model of parkinsonism. *J Neurophysiol*. 1994;72(2):507–520.
4. Hollerman JR, Grace AA. Subthalamic nucleus cell firing in the 6-OHDA-treated rat: basal activity and response to haloperidol. *Brain Res*. 1992; 590(1–2):291–299.
5. Benazzouz A, Boraud T, Feger J, Burbaud P, Bioulac B, Gross C. Alleviation of experimental hemiparkinsonism by high-frequency stimulation of the subthalamic nucleus in primates: a comparison with L-Dopa treatment. *Mov Disord*. 1996; 11(6):627–632.
6. Hassani OK, Mouroux M, Feger J. Increased subthalamic neuronal activity after nigral dopaminergic lesion independent of disinhibition via the globus pallidus. *Neuroscience*. 1996;72(1):105–115.
7. Perier C, Agid Y, Hirsch EC, Feger J. Ipsilateral and contralateral subthalamic activity after unilateral dopaminergic lesion. *Neuroreport*. 2000;11(14):3275–3278.
8. Vila M, et al. Evolution of changes in neuronal activity in the subthalamic nucleus of rats with unilateral lesion of the substantia nigra assessed by metabolic and electrophysiological measurements. *Eur J Neurosci*. 2000;12(1):337–344.
9. Bergman H, Wichmann T, DeLong MR. Reversal of experimental parkinsonism by lesions of the subthalamic nucleus. *Science*. 1990;249(4975):1436–1438.
10. Benazzouz A, Gross C, Féger J, Boraud T, Bioulac B. Reversal of rigidity and improvement in motor performance by subthalamic high-frequency stimulation in MPTP-treated monkeys. *Eur J Neurosci*. 1993;5(4):382–389.
11. Limousin P, et al. Bilateral subthalamic nucleus stimulation for severe Parkinson's disease. *Mov Disord*. 1995;10(5):672–674.
12. Krack P, Limousin P, Benabid AL, Pollak P. Chronic stimulation of subthalamic nucleus improves levodopa-induced dyskinesias in Parkinson's disease. *Lancet*. 1997;350(9092):1676.
13. Limousin P, et al. Electrical stimulation of the subthalamic nucleus in advanced Parkinson's disease. *N Engl J Med*. 1998;339(16):1105–1111.
14. Hamani C, Neimat JS, Lozano AM. Deep brain stimulation and chemical neuromodulation: current use and perspectives for the future. *Acta Neurochir*. 2007;97(pt 2):127–133.
15. Benabid AL, Chabardes S, Mitrofanis J, Pollak P. Deep brain stimulation of the subthalamic nucleus for the treatment of Parkinson's disease. *Lancet Neurol*. 2009;8(1):67–81.
16. Bevan MD, Wilson CJ. Mechanisms underlying spontaneous oscillation and rhythmic firing in rat subthalamic neurons. *J Neurosci*. 1999;19(17):7617–7628.
17. Do MT, Bean BP. Subthreshold sodium currents and pacemaking of subthalamic neurons: modulation by slow inactivation. *Neuron*. 2003;39(1):109–120.
18. Beurrier C, Bioulac B, Hammond C. Slowly inactivating sodium current (I(NaP)) underlies single-spike activity in rat subthalamic neurons. *J Neurophysiol*. 2000;83(4):1951–1957.
19. Nakanishi H, Kita H, Kitai ST. Electrical membrane properties of rat subthalamic neurons in an in vitro slice preparation. *Brain Res*. 1987;437(1):35–44.
20. Plenz D, Kital ST. A basal ganglia pacemaker formed by the subthalamic nucleus and external globus pallidus. *Nature*. 1999;400(6745):677–682.
21. Bevan MD, Magill PJ, Hallworth NE, Bolam JP, Wilson CJ. Regulation of the timing and pattern of action potential generation in rat subthalamic neurons in vitro by GABA-A IPSPs. *J Neurophysiol*. 2002;87(3):1348–1362.
22. Urbain N, Rentero N, Gervasoni D, Renaud B, Chouvet G. The switch of subthalamic neurons from an irregular to a bursting pattern does not solely depend on their GABAergic inputs in the anesthetic-free rat. *J Neurosci*. 2002;22(19):8665–8675.
23. Hallworth NE, Wilson CJ, Bevan MD. Apamin-sensitive small conductance calcium-activated potassium channels, through their selective coupling to voltage-gated calcium channels, are critical determinants of the precision, pace, and pattern of action potential generation in rat subthalamic nucleus neurons in vitro. *J Neurosci*. 2003; 23(20):7525–7542.
24. Baufreton J, et al. D5 (not D1) dopamine receptors potentiate burst-firing in neurons of the subthalamic nucleus by modulating an L-type calcium conductance. *J Neurosci*. 2003;23(3):816.
25. Cragg S, Baufreton J, Xue Y, Bolam J, Bevan M. Synaptic release of dopamine in the subthalamic nucleus. *Eur J Neurosci*. 2004;20(7):1788–1802.
26. Bal T, von Krosigk M, McCormick DA. Synaptic and membrane mechanisms underlying synchronized oscillations in the ferret lateral geniculate nucleus in vitro. *J Physiol*. 1995;483(pt 3):641–663.
27. Beurrier C, Congar P, Bioulac B, Hammond C. Subthalamic nucleus neurons switch from single-spike activity to burst-firing mode. *J Neurosci*. 1999;19(2):599.
28. Song W, Baba Y, Otsuka T, Murakami F. Characterization of Ca^{2+} channels in rat subthalamic nucleus neurons. *J Neurophysiol*. 2000;84(5):2630.
29. Lacinova L. Voltage-dependent calcium channels. *Gen Physiol Biophys*. 2005;24(suppl 1):1–78.
30. Perez-Reyes E. Molecular characterization of a novel family of low voltage-activated, T-type, calcium channels. *J Bioenerg Biomembr*. 1998;30(4):313–318.
31. Huguenard JR. Low-threshold calcium currents in central nervous system neurons. *Annu Rev Physiol*. 1996;58:329–348.
32. Clozel JP, Ertel EA, Ertel SI. Discovery and main pharmacological properties of mibefradil (Ro 40-5967), the first selective T-type calcium channel blocker. *J Hypertens Suppl*. 1997;15(5):S17–S25.
33. Lee JH, Gomora JC, Cribbs LL, Perez-Reyes E. Nickel block of three cloned T-type calcium channels: low concentrations selectively block alpha1H. *Biophys J*. 1999;77(6):3034–3042.
34. Monteil A, Chemin J, Bourinet E, Mennessier G, Lory P, Nargeot J. Molecular and functional properties of the human alpha(1G) subunit that forms T-type calcium channels. *J Biol Chem*. 2000;275(9):6090–6100.
35. Klugbauer N, Marais E, Lacinova L, Hofmann F. A T-type calcium channel from mouse brain. *Pflugers Arch*. 1999;437(5):710–715.
36. Magarinos-Ascone C, Pazo JH, Macadar O, Buno W. High-frequency stimulation of the subthalamic nucleus silences subthalamic neurons: a possible cellular mechanism in Parkinson's disease. *Neuroscience*. 2002;115(4):1109–1117.
37. Huang L, et al. NNC 55-0396 [(1S,2S)-2-(2-(N-[(3-benzimidazol-2-yl)propyl]-N-methylamino)ethyl)-6-fluoro-1,2,3,4-tetrahydro-1-isopropyl-2-naphtyl cyclopropanecarboxylate dihydrochloride]: a new selective inhibitor of T-type calcium channels. *J Pharmacol Exp Ther*. 2004;309(1):193–199.
38. Li M, Hansen JB, Huang L, Keyser BM, Taylor JT. Towards selective antagonists of T-type calcium channels: design, characterization and potential applications of NNC 55-0396. *Cardiovasc Drug Rev*. 2005;23(2):173–196.
39. Bui PH, Quesada A, Handforth A, Hankinson O. The mibefradil derivative NNC55-0396, a specific T-type calcium channel antagonist, exhibits less CYP3A4 inhibition than mibefradil. *Drug Metab Dispos*. 2008;36(7):1291–1299.
40. Lacinova L, Klugbauer N, Hofmann F. Regulation of the calcium channel alpha(1G) subunit by divalent cations and organic blockers. *Neuropharmacology*. 2000;39(7):1254–1266.
41. Perchenet L, Benardeau A, Ertel EA. Pharmacologi-

cal properties of Ca(V)3.2, a low voltage-activated Ca^{2+} channel cloned from human heart. *Naunyn Schmiedebergs Arch Pharmacol*. 2000;361(6):590–599.
42. Furukawa T, et al. Identification of R(-)-isomer of efonidipine as a selective blocker of T-type Ca^{2+} channels. *Br J Pharmacol*. 2004;143(8):1050–1057.
43. Shin MC, Kim CJ, Min BI, Ogawa S, Tanaka E, Akaike N. A selective T-type Ca^{2+} channel blocker R(-) efonidipine. *Naunyn Schmiedebergs Arch Pharmacol*. 2008;377(4–6):411–421.
44. Lenz FA, Kwan HC, Martin RL, Tasker RR, Dostrovsky JO, Lenz YE. Single unit analysis of the human ventral thalamic nuclear group. Tremor-related activity in functionally identified cells. *Brain*. 1994;117(pt 3):531–543.
45. Volkmann J, et al. Central motor loop oscillations in parkinsonian resting tremor revealed by magnetoencephalography. *Neurology*. 1996;46(5):1359–1370.
46. Hurtado JM, Gray CM, Tamas LB, Sigvardt KA. Dynamics of tremor-related oscillations in the human globus pallidus: a single case study. *Proc Natl Acad Sci U S A*. 1999;96(4):1674–1679.
47. Elble RJ. Origins of tremor. *Lancet*. 2000; 355(9210):1113–1114.
48. Timmermann L, Gross J, Dirks M, Volkmann J, Freund HJ, Schnitzler A. The cerebral oscillatory network of parkinsonian resting tremor. *Brain*. 2003;126(pt 1):199–212.
49. Amtage F, et al. Tremor-correlated neuronal activity in the subthalamic nucleus of Parkinsonian patients. *Neurosci Lett*. 2008;442(3):195–199.
50. Reck C, et al. Characterisation of tremor-associated local field potentials in the subthalamic nucleus in Parkinson's disease. *Eur J Neurosci*. 2009; 29(3):599–612.
51. Bergman H, Wichmann T, Karmon B, DeLong M. The primate subthalamic nucleus. II. Neuronal activity in the MPTP model of parkinsonism. *J Neurophysiol*. 1994;72(2):507.
52. Alvarez L, et al. Therapeutic efficacy of unilateral subthalamotomy in Parkinson's disease: results in 89 patients followed for up to 36 months. *J Neurol Neurosurg Psychiatry*. 2009;80(9):979–985.
53. Perez-Reyes E, et al. Molecular characterization of a neuronal low-voltage-activated T-type calcium channel. *Nature*. 1998;391(6670):896–900.
54. Kuo CC, Yang S. Recovery from inactivation of t-type Ca^{2+} channels in rat thalamic neurons. *J Neurosci*. 2001;21(6):1884–1892.
55. Carlson JD, Cleary DR, Cetas JS, Heinricher MM, Burchiel KJ. Deep brain stimulation does not silence neurons in subthalamic nucleus in Parkinson's patients. *J Neurophysiol*. 2010; 103(2):962–967.
56. Benazzouz A, Hallett M. Mechanism of action of deep brain stimulation. *Neurology*. 2000; 55(12 suppl 6):S13–S16.
57. Nambu A. A new approach to understand the pathophysiology of Parkinson's disease. *J Neurol*. 2005;252(suppl 4):IV1–IV4.
58. Akaike N. [Physiology and pharmacology of calcium channel]. *Nippon Seirigaku Zasshi*. 1983;45(6):261–278.
59. Carbone E, Lux HD. Kinetics and selectivity of a low-voltage-activated calcium current in chick and rat sensory neurones. *J Physiol*. 1987;386:547–570.
60. Paxinoa G, Watson C. *The Rat Brain in Stereotaxic Coordinates*. 3rd ed. San Diego, California, USA: Academic Press; 1996.